Photo source: Derek Ray (NHC)

Haida Gwaii Coastal Flood and Erosion Study
Appendix B – Metocean Conditions

Prepared by:

Northwest Hydraulic Consultants Ltd.
30 Gostick Place
North Vancouver, BC V7M 3G3
Tel: (604) 980-6011
www.nhcweb.com

NHC Project Contact:
Grant Lamont, PEng, MASc
Principal, Senior Coastal Engineer

December 7, 2022
Final Report, Rev. 2

NHC Reference 3006196

Prepared for:

North Coast Regional District
(representing the communities of Tlell and Sandspit)
14 – 342 3rd Avenue West
Prince Rupert, BC V8J 1L5

In association with:
Village of Masset
Village of Port Clements
Village of Daajing Giids
Haida Gwaii, BC

Document Tracking

Date	Revision No.	Reviewer	Issued for
December 2, 2022	0	Grant Lamont, Derek Ray	Draft for client comments
December 7, 2022	1	Grant Lamont, Derek Ray	Draft for client review
December 23, 2022	2	Grant Lamont, Derek Ray	Final

Appendix prepared by:

Logan Ashall, EIT, MASc	Project Coastal Specialist
Philippe St-Germain, PEng, MASc	Coastal Engineer

Appendix reviewed by:

Grant Lamont, PEng, MASc	Principal, Coastal Engineer
Derek Ray, PGeo, MSc	Principal, Senior Geomorphologist

EGBC Permit to Practice No.: *1003221*

DISCLAIMER

This report has been prepared by **Northwest Hydraulic Consultants Ltd.** for the benefit of the **North Coast Regional District**, the **Village of Masset**, the **Village of Port Clements**, and the **Village of Daajing Giids** for specific application to the Haida Gwaii Coastal Flood and Erosion Study. The information and data contained herein represent **Northwest Hydraulic Consultants Ltd.'s** best professional judgement in light of the knowledge and information available to **Northwest Hydraulic Consultants Ltd.** at the time of preparation and was prepared in accordance with generally accepted engineering and geoscience practices.

Except as required by law, this report and the information and data contained herein may be used and relied upon only by **North Coast Regional District**, the **Village of Masset**, the **Village of Port Clements**, and the **Village of Daajing Giids**, their officers and employees. **Northwest Hydraulic Consultants Ltd.** denies any liability whatsoever to other parties who may obtain access to this report for any injury, loss, or damage suffered by such parties arising from their use of or reliance upon this report or any of its contents.

EXECUTIVE SUMMARY

All residents of Haida Gwaii live in shoreline communities and depend on critical infrastructure that is subject to flooding and erosion from ocean processes. Each community is increasingly vulnerable to rising sea levels, as shown by the ongoing shoreline issues currently affecting the community of Tlell, when high tides coincide with large windstorms. Shoreline erosion is now occurring at several locations and will accelerate and expand to affect more of the coastline, as higher sea levels promote the effects of the waves reaching higher up on the shoreline.

Northwest Hydraulic Consultants Ltd. (NHC) and Ocean Networks Canada Society have been engaged to provide professional engineering, geoscience, and oceanographic consulting services for five communities in Haida Gwaii, British Columbia. This study on coastal flooding and erosion examines the effects of wind waves and tsunamis when combined with sea-level rise. The team was selected following a successful proposal submission in response to the Joint Request for Proposal No. 2020-02 issued by the North Coast Regional District, in association with the Village of Masset, the Village of Port Clements, and the Village of Daajing Giids[1]. For the purposes of this study, the communities of Tlell and Sandspit are represented by the North Coast Regional District.

This report provides a summary of the meteorological and oceanographic (metocean) analysis to better understand the governing conditions offshore from Haida Gwaii. These results inform the overall study conclusions, which are described in the main report, *Haida Gwaii Coastal Flood and Erosion Study – Planning for Sea-Level Rise and Tsunami Hazard*. The metocean conditions described in this report and summarized below are used as inputs for modelling coastal storm flood hazards and presented in Appendix C. Please refer to the main report for background information about the project, including a statement of the objectives under investigation, the project goals, and the methodology used to conduct the analysis.

Water Levels

Coastal water levels are influenced by multiple variables such as astronomical tides, wind, atmospheric pressure, temperature, and salinity. The variables with the greatest influence are astronomical tides as well as wind and atmospheric pressure, which when combined, produce storm surge. Tides in Dixon Entrance and Hecate Strait are mixed semidiurnal, and the tidal range, which corresponds to the difference in height between the highest high tide and lowest low tide, varies across the coastlines of Haida Gwaii.

At Langara Point, located to the northwest of Graham Island, the tidal range is 5.2 m. At Daajing Giids in Skidegate Inlet, the tidal range is 7.7 m, which is the largest range recorded in Haida Gwaii. The length, width, and relatively shallow depth of Masset Sound directly affect the propagation of the tide. As such, the tidal range in Masset Sound is smaller than in McIntyre Bay due to the constricting physical characteristics of the sound's channel. The tidal range at the entrance of Delkatla Inlet in the Village of Masset is 4.3 m in comparison to 6.0 m at Wiah Point, which is located just west of McIntyre Bay in Dixon Entrance. As the distance increases from McIntyre Bay toward Masset Inlet, the tidal range and the height of high tides are further reduced, with the tidal range at Port Clements and Juskatla

[1] The Village of Daajing Giids was formally named the Village of Queen Charlotte and Queen Charlotte City before then.

measured at 3.0 m and 1.9 m, respectively. The tidal ranges at Daajing Giids and the communities of Tlell and Sandspit are similar, varying from 7.4 to 7.7 m.

While tides are driven by astronomical forcing, storm surges occur because of atmospheric forcing, which combines the effects of the wind and atmospheric pressure associated with storm systems. Storm surge is calculated based on the residual water level, which is the difference between the measured or observed water level and the predicted astronomical tide. For this study, NHC calculated long-term records of storm surge for Langara Island (Dixon Entrance) and the Village of Daajing Giids (Hecate Strait). Results show that storm surge in Hecate Strait tends to be higher than in Dixon Entrance.

Wind Regime

Winds blowing over water generate waves by transferring energy to the water surface through friction. It is therefore necessary to accurately characterize offshore winds to reliably estimate the wave climate in the study area. Storm systems in this region of the northeastern Pacific are characterized by seasonably opposed winds that are strongest in the winter months. According to Walker and Barrie (2006), the Aleutian Low develops and intensifies, causing a counter-clockwise circulation of low-altitude winds. From October through April, this low-pressure system brings southerly and southeasterly winds up Hecate Strait and over Haida Gwaii in general. With the arrival of spring, the Aleutian Low declines and retreats to the northwest, while the North Pacific High expands and intensifies, which shifts the dominant southeasterly winds to a northwesterly direction, which dominates in the summer.

The data from measuring stations show that the predominant winds are from the southeast in both Dixon Entrance and Hecate Strait, although strong winds (e.g., > 17.5 metres per second or gale force) are more frequent in Hecate Strait in comparison to Dixon Entrance. Strong westerly winds can occur in Dixon Entrance, and strong northerly winds can also occur in Hecate Strait, although they occur less frequently.

Offshore Wave Climate

NHC analyzed historical wave observations measured at several offshore wave buoys to characterize the general wave conditions inside Dixon Entrance and Hecate Strait. Such measurements include wave height and wave period, but not wave direction. Since it is important to distinguish where the sector waves originate from to establish statistics, the team conducted additional analysis to infer wave direction from available metocean parameters. The wave conditions are analyzed further in Appendix C, which presents the wave modelling undertaken to understand how offshore waves propagate toward and affect the shorelines of the study areas.

Waves generated locally by wind are known as wind sea. On large bodies of water, such as the open ocean, waves will travel beyond the area in which they are generated. Such waves are called swell. While the waves travel over long distances, their frequencies are reorganized, and the waves become more orderly, with the waves of similar frequency (i.e., wave period) being grouped together to form a wave train. Swell tends to have longer wave periods in comparison to wind sea, which means the energy associated with swell is greater, even for waves of equal height. A transitional sea is described as a swell over which locally generated wind waves are also present to some degree. NHC determined that westerly swell conditions for Dixon Entrance are predominant in comparison to wind sea conditions coming from the east. In Hecate Strait, the occurrence of wind sea from the northern sector is relatively rare in comparison to stronger transitional sea coming from the southern sector.

Joint Probability Analysis

In a coastal environment, static water level and wave height are both factors in damage inflicted on a coastline. The extent of damage may vary, depending on combinations of these two oceanographic parameters. NHC conducted a joint probability analysis to establish various combinations of water level and wave heigh to confirm which combination results in the most adverse conditions at the study areas' shorelines.

TABLE OF CONTENTS

LIST OF TABLES

LIST OF FIGURES

ABBREVIATIONS

Acronym / Abbreviation	Definition
ERA5	Fifth generation atmospheric reanalysis of the global climate by the European Centre for Medium-Range Weather Forecasts
AEP	annual exceedance probability
BC	British Columbia
CD	chart datum
CHS	Canadian Hydrographic Service
CGVD2013	Canadian geodetic vertical datum of 2013
DEE	Dixon Entrance eastern sector of wind and wave exposure
DEW	Dixon Entrance western sector of wind and wave exposure
DFO	Fisheries and Oceans Canada
ECCC	Environment and Climate Change Canada
FLNRORD	BC Ministry of Forests, Natural Resource Operations and Rural Development[2]
HHWLT	higher high-water, large tide
HHWMT	higher high-water, mean tide
HRDPS	High-resolution Deterministic Prediction System
HSN	Hecate Strait northern sector of wind and wave exposure
HSS	Hecate Strait southern sector of wind and wave exposure
metocean	meteorological and oceanographic
MWL	mean water level
LLWLT	lower low-water, large tide
LLWMT	lower low-water, mean tide
NHC	Northwest Hydraulic Consultants Ltd.
US	United States of America
USACE	US Army Corps of Engineers

[2] This ministry has undergone many name changes including the most recent in April 2022, which created two new ministries. Namely, the Ministry of Forests and the Ministry of Land, Water and Resource Stewardship.

SYMBOLS AND UNITS OF MEASURE

Symbol / Unit of Measure	Definition
>	greater than
<	less than
°	degree
°T	the direction in degrees with respect to true north, measured clockwise
H_s	significant wave height
km	kilometre
km^2	square kilometre
m	metre
m/s	metres per second
s	wave steepness
sec	second
T_p	peak wave period

GLOSSARY

Term	Definition
Aleutian Low	A semi-permanent, subpolar area of low pressure located in the Gulf of Alaska near the Aleutian Islands during winter in the Northern Hemisphere. It is a generating area for storms and migratory lows, such as extratropical cyclones, which form in the subpolar latitudes, often reaching maximum intensity in this area.
anemometer	A device that measures wind speed and direction.
anticyclone	A weather phenomenon defined as a large-scale circulation of winds around a central region of high atmospheric pressure, clockwise in the Northern Hemisphere and counter-clockwise in the Southern Hemisphere as viewed from above (opposite to a cyclone).
annual exceedance probability	The probability that a given event will be exceeded in any one year.
astronomical forcing	Influence that is driven by forces associated with atmospheric phenomena.
astronomical tides	The tidal levels and water motion resulting from the earth's rotation and the gravitational effects of the earth, sun, and moon in particular, without any atmospheric influences.
atmospheric forcing	Influence that is driven by forces associated with atmospheric phenomena.
Canadian Geodetic Vertical Datum of 1928	A vertical datum defined by the mean water level at five tide gauges: Yarmouth and Halifax on the Atlantic Ocean, Pointe-au-Père on the St. Lawrence River, and Vancouver and Prince Rupert on the Pacific Ocean.
Canadian Geodetic Vertical Datum of 2013	Reference standard for heights across Canada. This height reference system replaced the Canadian Geodetic Vertical Datum of 1928 and is defined by a surface of equal gravitational potential (equipotential surface), which represents, by convention, the coastal mean sea level for North America.
chart datum	For navigational safety, depths on a chart are shown from a low-water surface or a low-water datum. Chart datum is selected so that the water level will seldom fall below it and rarely with less depth available than what is portrayed on the chart. On most Canadian coastal charts, the surface of lower low-water, large tide (also known as LLWLT) has been adopted as chart datum.
continental shelf	A portion of a continent that is submerged under an area of relatively shallow water, known as a shelf.
cyclone	A large air mass that rotates around a strong centre of low atmospheric pressure, counter-clockwise in the Northern Hemisphere and clockwise in the Southern Hemisphere as viewed from above.

extreme value frequency analysis	The study of the probability of occurrence of events. This term is often used in regulatory contexts to determine design values for infrastructure.
fetch	The length of an ocean's or lake's surface over which the wind blows in an essentially constant direction, thus generating waves.
fetch-limited	A situation in which wave height is limited by the length of the fetch available for wave generation from a particular direction.
gale force	According to the Beaufort wind scale, gale force corresponds to wind speeds in the range of 34 to 40 knots (17.5 to 20.5 m/s) that generate moderately high waves of greater length; the edges of wave crests break into spindrift; foam is blown in well-marked streaks along the direction of the wind.
higher high-water, large tide	The average of the yearly highest high tides predicted from each year over a tidal epoch, as defined by the Canadian Hydrographic Service (CHS) in Canada.
higher high-water, mean tide	The average of the higher high-water height of each tidal day observed over a tidal epoch, as defined by the CHS in Canada.
joint probability	A statistical measure that calculates the likelihood of two events occurring together and at the same point in time.
lower low-water, large tide	The average of the yearly lowest low tide tides predicted from each year over a tidal epoch, as defined by the CHS in Canada.
lower low-water, mean tide	The average of the lower low-water height of each tidal day observed over a tidal epoch, as defined by the CHS in Canada.
mean water level	The average of all water levels over the available period of record.
Monte Carlo method	A way to use random samples of parameters to explore the behaviour of a complex system.
North Pacific High	A semi-permanent, subtropical anticyclone located in the northeastern portion of the Pacific Ocean, located northeast of Hawaii and west of California. It is strongest in the Northern Hemisphere during the summer and shifts toward the equator during the winter.
Pareto distribution	A power-law probability distribution used to describe social, quality control, scientific, geophysical, actuarial, and other types of observable phenomena.
peak-over-threshold analysis	Analysis that involves identifying events that exceed a certain threshold.
peak wave period	The wave period (in seconds) associated with the most energetic waves in the total wave spectrum at a specific location.
percentile	Each of the 100 equal groups into which a statistical population (i.e., sample) can be divided according to the distribution of values of a particular variable.

reference port	A location with tidal heights that are directly given in the tide tables. The tidal heights for reference ports are based on continuous observation of tide over a longer period.
residual water level	The part of the sea level that remains once the astronomical tidal component has been removed.
secondary port	A location with tidal heights that are not given directly in tide tables and must be calculated based on the tidal heights of a reference port.
significant wave height	The mean height of the highest one-third of all waves.
spindrift	The spray that blows from the wind over the crests of waves.
storm surge	Occurs in coastal areas during passing storms when strong onshore winds and low atmospheric pressure raise water levels along the shore above predicted levels.
subduction zone	The place where two tectonic plates collide, with one plate sinking into the earth's mantle underneath the other plate.
swell	Wind waves that have travelled some distance away from the area where they were generated. Swell waves often feature relatively smooth, long wave lengths with more regular and uniform crests, which typically carry more energy.
tidal harmonic constituents	The harmonic elements in a mathematical expression for the tide producing force and in the corresponding formula for the tidal curve. Each constituent represents a periodic change or variation in the relative positions of celestial bodies such as the earth, moon, and sun.
tidal height	The vertical distance the water rises or falls due to the tide. Standard heights are published by the CHS in Canadian waters, which are established statistically.
tidal range	The difference in height between the highest high tide and the lowest low tide at one location.
total water level	The observed water level measured by tide gauges, which includes a combination of astronomical tides, storm surge, and local wind and wave setup, if present.
transitional sea	A swell over which locally generated wind waves are also present.
true north	The direction that points directly toward the geographic North Pole, which may vary from the magnetic north.
tsunami	A series of travelling ocean waves of extremely long length and period, triggered by a large earthquake occurring near or under the ocean, a volcanic eruption, or a submarine landslide or onshore landslide.
wave height	The vertical distance between the crest and the trough of a wave.
wave period	The time it takes for two successive crests or one wavelength to pass a specified location.

wave setup	The increase in the mean water level in a shoreward area due to the influx of breaking waves against the beach.
wave steepness	The ratio of wave height to wavelength.
wind rose	A diagram used to show wind magnitude, direction, and frequency. Each stem in the diagram characterizes the wind coming from the direction in which it expands outward; the individual length of the coloured segments along a stem represents the frequency of the wind within a specific speed range.
wind sea	Waves under the influence of local winds that generate them.
wind waves	Waves that occur on the surface of waterbodies water as a results from the wind blowing over the water surface.

1 INTRODUCTION

All residents of Haida Gwaii live in shoreline communities and depend on critical infrastructure that is subject to flooding and erosion from ocean processes. Each community is increasingly vulnerable to rising sea levels, as shown by the ongoing shoreline issues currently affecting the community of Tlell, when high tides coincide with large windstorms. Shoreline erosion is now occurring at several locations and will accelerate and expand to affect more of the coastline, as higher sea levels promote the effects of the waves reaching higher up on the shoreline. Furthermore, many residents are at risk of being affected by **tsunamis**, particularly given the island's exposure to the Alaska-Aleutian and the Cascadia **subduction zones**.

Northwest Hydraulic Consultants Ltd. (NHC) and Ocean Networks Canada Society have been engaged to provide professional engineering, geoscience, and oceanographic consulting services for five communities in Haida Gwaii, British Columbia (BC). This study on coastal flooding and erosion examines the effects of **wind waves** and tsunamis combined with sea-level rise. The team was selected following a successful proposal submission in response to the Joint Request for Proposal No. 2020-02 issued by the North Coast Regional District, in association with the Village of Masset, the Village of Port Clements, and the Village of Daajing Giids[3]. For the purposes of this study, the communities of Tlell and Sandspit are represented by the North Coast Regional District.

This report provides a summary of the meteorological and oceanographic (metocean) analysis to better understand the governing conditions offshore of Haida Gwaii. These results inform the overall study conclusions, which are described in the main report, *Haida Gwaii Coastal Flood and Erosion Study – Planning for Sea-Level Rise and Tsunami Hazard*. The metocean conditions described in this report are used as inputs for modelling coastal storm flood hazards and presented in Appendix C. Please refer to the main report for background information about the project, including a statement of the objectives under investigation, the project goals, and the methodology used to conduct the analysis.

1.1 Study Areas

The areas of Haida Gwaii that are covered under the scope of this study include the following communities, from north to south and west to east:

- the Village of Masset and its jurisdiction
- the community of Tow Hill
- the Village of Port Clements and its jurisdiction
- the community of Tlell and neighbouring shoreline
- the Village of Daajing Giids and its jurisdiction
- the community of Sandspit

[3] The Village of Daajing Giids was formally named the Village of Queen Charlotte and Queen Charlotte City before then.

The spatial extents of the study areas are shown in Figure 1-1. It should be noted that the assessment at Tow Hill is limited to tsunami hazards only, which are not discussed in this document but in the project's main report.

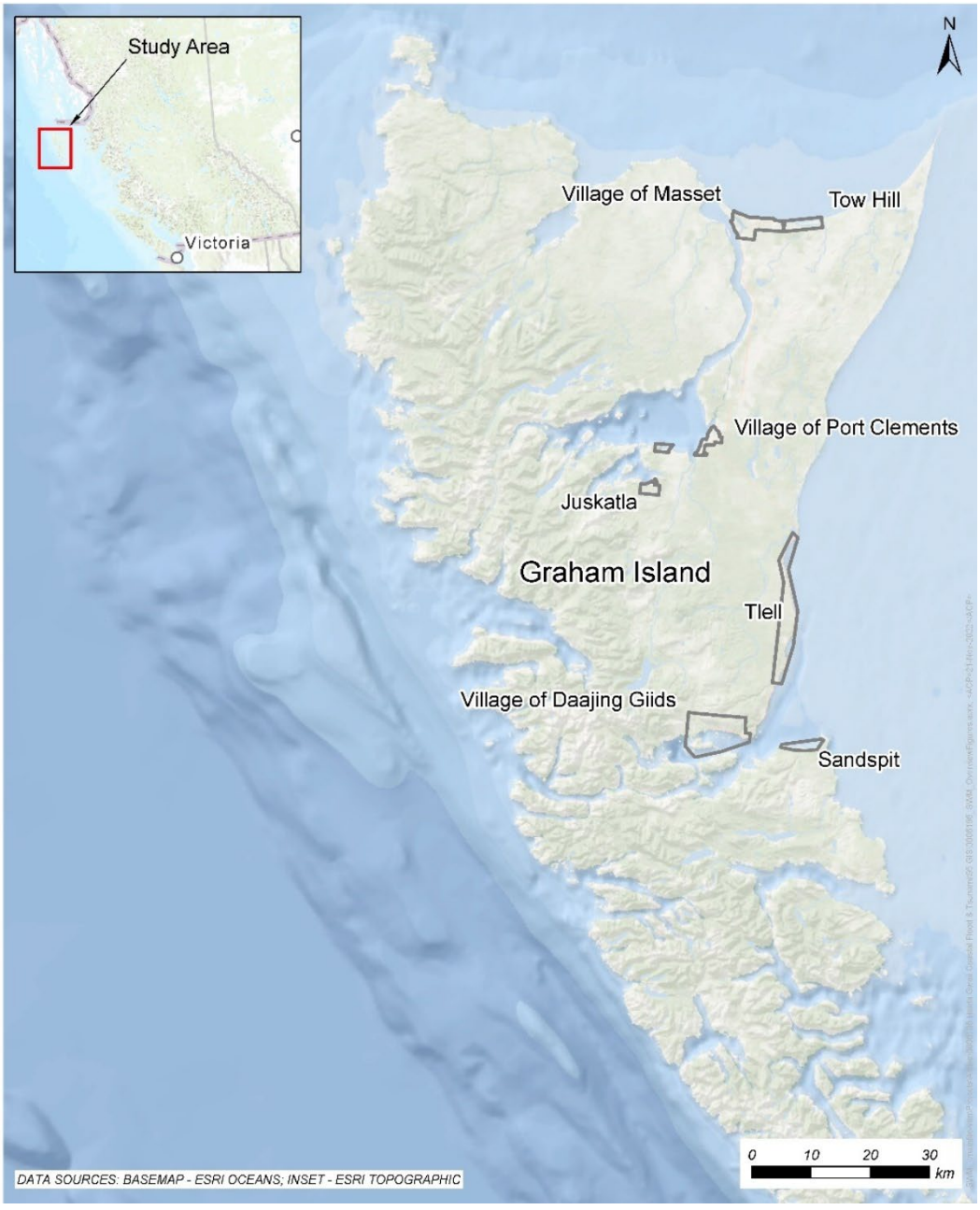

Figure 1-1. Areas of Haida Gwaii included in this project, shown with a grey perimeter. The location of the broader study area is shown with a red perimeter in the inset.

1.2 Physical Setting

Defined in Haida language as *X̲aaydaga Gwaay.yaay / X̲aayda gwaay*, which translates to "Islands of the Haida people," Haida Gwaii is an island archipelago located off the northern coast of BC. The overall land mass is primarily contained in the two largest of the approximately 150 islands that make up Haida Gwaii. Graham Island and Moresby Island are separated by the narrow Skidegate Channel, which extends west from Skidegate Inlet. The total land area is approximately 9,945 square kilometres (km^2);h Graham Island is approximately 6,436 km^2 and Moresby Island is 2,745 km^2. Located at the centre of Graham Island, Masset Inlet is a large saltwater bay. Approximately 30 km long and 15 km wide and with depths varying between 20 and 100 m, the inlet is fed by several rivers and is connected to McIntyre Bay by the narrow Masset Sound. This channel is 38 km long and 1.5 km wide on average, with depths varying between 10 and 25 m.

The waters surrounding Haida Gwaii's shorelines are described as four separate bodies based on their physiological characteristics: Dixon Entrance to the north, Hecate Strait to the east, Queen Charlotte Sound to the south, and the Pacific Ocean to the west (Figure 1-2).

Dixon Entrance is an inlet approximately 140 km long by 80 km wide and forms part of the maritime boundary between Canada and the state of Alaska in the United States (US), with depths varying between 200 and 500 m. Hecate Strait, which separates Haida Gwaii from the BC mainland, is a relatively wide, shallow waterbody, in which depths generally vary from 20 to 100 m. The strait is approximately 260 km in length on a roughly north-south axis and is 140 km wide where it merges with Queen Charlotte Sound to the south before narrowing to approximately 48 km where it meets Dixon Entrance to the north.

Queen Charlotte Sound is located between Vancouver Island to the south and Haida Gwaii to the north, which are approximately 200 km apart. The sound, which extends approximately 150 km offshore from the mainland, is bounded to the west by the outer fringe of the **continental shelf** where the water depth drops below 1,000 m.

Figure 1-2. The ocean water bodies surrounding Haida Gwaii.

1.3 Measurement Stations

The metocean analysis for the study uses data from measurement stations located in Haida Gwaii and within the surrounding water bodies, as shown in Figure 1-3. The data gathered from these stations include the following:

- long-term ocean water levels measured by tide gauges operated by the Canadian Hydrographic Service (CHS)
- wind speed and wind direction recorded at meteorological stations operated by Environment and Climate Change Canada (ECCC)
- **wave height** and **wave period** as well as wind speed and wind direction measured at offshore wave buoys operated by Fisheries and Oceans Canada (DFO)

Additional details regarding these stations and the information they provide are presented in the sections that follow.

Figure 1-3. Location of measurement stations considered for the project's metocean analysis.

1.4 Glossary of Terms

The main report includes a glossary of terms that are specialized to the coastal processes field of study and essential for preserving accuracy in descriptions. The terms included in the glossary are set in bold when they first appear in the text.

2 WATER LEVELS

This section describes the water levels on the coast of Haida Gwaii and includes discussions of stations where the CHS reports tidal information and provides information on **tidal heights** and **storm surge**. In CHS publications these stations are referred to as **reference ports** and **secondary ports**, as explained below.

2.1 Tide Gauge Measurements

The CHS uses water level measurements collected at tide gauges to derive **tidal harmonic constituents**, which in turn can be used to accurately predict future (and past) tides and establish tidal heights. Locations where long-term measurements are available are typically reference ports; tidal heights at secondary ports are obtained by applying simple adjustments to the tidal heights reported at reference ports. Water level measurements at secondary ports are required to derive harmonic constituents for tide prediction and to establish the adjustments to determine tidal heights based on reference ports, but these measurements are generally temporary (in effect for several years) and are not long enough to use in statistical analysis.

NHC analyzed water level measurements to assess both storm surge and the **joint probability** of tide, storm surge, and waves combined. Results of such analyses are presented in Section 2.3 and Section 5, respectively. NHC considered the tide gauges of the reference ports of the Village of Dajing Giids and Langara Point for the analysis. Table 2-1 summarizes the period of record for these stations.

The tide gauge at the reference port of Langara Point was in operation until 2007, which approximately coincides with the period when the tide gauge at the secondary port in Henslung Cove entered operation. These two stations are located close to one another (within 2 km), and the difference in tidal heights is small (less than 0.1 m). To create a longer period of record that is representative of water levels at Langara Island, NHC merged the measurements from these two stations, thus enabling a more meaningful statistical analysis.

Table 2-1. Period of records of water level measurements considered for the project analysis.

Location	CHS Station No.	Latitude	Longitude	Year Start	Year End	Data Missing
Village of Daajing Giids[1]	9850	53° 15’	132° 04’	1964	Present	-
Langara Point[2]	9964	54° 15’	133° 02’	1973	2007	1984 – 2001, 2003 – 2006
Henslung Cove	9958	54° 11’	133° 00’	2006	Present	2014

Notes: 1. The reference port at the Village of Daajing Giids is listed as “Queen Charlotte” or “Queen Charlotte City” in CHS publications.

2. The operation of the tide gauge at this reference port ceased.

2.2 Tidal Heights

Since **astronomical tides** are influenced by the cyclic movement of celestial bodies and are not influenced by weather, astronomical tides can be accurately predicted. The astronomical tide conditions presented below for the various study areas are based on the tidal height information provided in the Canadian tide and current tables (CHS, 2022).

2.2.1 Masset

The jurisdiction of the Village of Masset has shorelines extending within Masset Sound to the west as well as in McIntyre Bay to the north. The **tidal range** in Masset Sound is smaller than in McIntyre Bay due to the constricting physical characteristics of the sound's channel. The tidal range at the secondary port located near the entrance of Delkatla Inlet in the Village of Masset is 4.3 m, in comparison to 6.0 m at the secondary port at Wiah Point, which is located just west of McIntyre Bay in Dixon Entrance. Tidal heights published for Masset (CHS station no. 9910) and Wiah Point (CHS station no. 9940) are provided in Table 2-2.

Table 2-2. Tidal heights at the secondary ports considered for the Village of Masset jurisdiction.

Tidal Height[1]	Masset (m, CGVD2013)	Wiah Point (m, CGVD2013)
Higher high-water, large tide (HHWLT)	2.5	3.0
Higher high-water, mean tide (HHWMT)	1.7	2.0
Mean water level (MWL)	0.3	0.1
Lower low-water, mean tide (LLWMT)	-1.2	-1.9
Lower low-water, large tide (LLWLT)	-1.8	-3.0

Notes: 1. The local conversion from the **Canadian geodetic vertical datum of 2013** (CGVD2013) to **chart datum** (CD) is +1.70 m at Masset and +3.08 m at Wiah Point as per CHS benchmarks no. 11-1964 and M17C9029, respectively.

2.2.2 Port Clements

The length, width, and relatively shallow depth of Masset Sound directly affects the propagation of the tide, which is why the tidal range reduces with the distance away from McIntyre Bay. As such, the tidal range at Port Clements is 3.0 m in comparison to 4.3 m at Masset, which is situated further north in the sound. Table 2-3 provides published tidal heights for the secondary ports located at Port Clements (CHS station no. 9920) and Juskatla (CHS station no. 9927).

Table 2-3. Tidal heights at the secondary ports considered for the Village of Port Clements jurisdiction.

Tidal Height	Port Clements (m, CGVD2013)	Juskatla (m, CGVD2013)
HHWLT	1.8	0.7
HHWMT	1.2	0.3
MWL	0.1	-0.4
LLWMT	-1.0	-1.0
LLWLT	-1.2	-1.2

Notes: 1. The local conversion from Canadian geodetic vertical datum of 2013 (CGVD2013) to chart datum (CD) is +1.16 m at Port Clements as per CHS benchmark no. M17C9045. This conversion is considered the same for Juskatla.

2.2.3 Tlell

Table 2-4 provides published tidal heights for the secondary port located at the community of Tlell (CHS station no. 9860).

Table 2-4. Tidal heights at the secondary port considered for the community of Tlell.

Tidal Height	Tlell (m, CGVD2013)
HHWLT	3.6
HHWMT	2.4
MWL	0.1
LLWMT	-2.4
LLWLT	-3.8

Notes: 1. The local conversion from Canadian geodetic vertical datum of 2013 (CGVD2013) to chart datum (CD) is +3.68 m at Tlell as per CHS benchmark no. M18C9009.

2.2.4 Daajing Giids

The reference port located at the Village of Daajing Giids (CHS station no. 9850) experiences a tidal range of 7.7 m, which is the largest range for all Haida Gwaii. Table 2-5 provides published tidal heights for Daajing Giids.

Table 2-5. Tidal heights at the reference port considered for the Village of Daajing Giids.

Tidal Height	Daajing Giids (m, CGVD2013)
HHWLT	3.7
HHWMT	2.4
MWL	0.1
LLWMT	-2.6
LLWLT	-4.0

Notes: 1. The local conversion from Canadian geodetic vertical datum of 2013 (CGVD2013) to chart datum (CD) is +3.88 m at Daajing Giids as per CHS benchmark M09C9004.
2. The reference port at the Village of Daajing Giids is listed as "Queen Charlotte" or "Queen Charlotte City" in CHS publications.

2.2.5 Sandspit

Table 2-6 provides published tidal heights for secondary port located in Shingle Bay (CHS station no. 9808) just west of the community of Sandspit.

Table 2-6. Tidal heights at the secondary port considered for the community of Sandspit.

Tidal Height	Shingle Bay (m, CGVD2013)
HHWLT	3.7
HHWMT	2.6
MWL	0.2
LLWMT	-2.5
LLWLT	-3.7

Notes: 1. The local conversion from Canadian geodetic vertical datum of 2013 (CGVD2013) to chart datum (CD) is +3.84 m at Sandspit as per CHS benchmark no. M18C9022.

2.3 Storm Surge

While tides are driven by **astronomical forcing**, storm surges occur because of **atmospheric forcing**, which combines the effects of the wind and atmospheric pressure. Excluding the local effect of storm waves (i.e., **wave setup**), the total observed water level near the coast during a storm is formed by adding the storm surge to the astronomical tide. These two components are independent from one another, since they are independently driven by distinct and unrelated forcing mechanisms.

Storm surge is calculated based on the **residual water level**, which is the difference between the measured or observed water level and the predicted astronomical tide. For this study, NHC calculated long-term records of storm surge for Langara Island (Dixon Entrance) and the Village of Daajing Giids (Hecate Strait) based on measurement records kept over 49 and 58 years, respectively.

Considering the entire duration of the available records, NHC computed storm surges with varying **annual exceedance probability** (AEP) using a Fisher-Tippett type I (Gumbel) probability distribution method, based on an analysis of peak-over-threshold values. Results are presented in Table 2-7 for both Langara Island and the Village of Daajing Giids.

Table 2-7. Storm surge of varying AEP for Langara Island and the Village of Daajing Giids.

AEP (%)	Storm Surge (m)	
	Langara Island	Daajing Giids
0.5	0.78	1.40
1	0.73	1.33
2	0.69	1.26
5	0.63	1.17
20	0.53	1.03
Annual	0.40	0.82

To get a general sense of the water levels observed during a storm, the surge is added to the tide level. Tidal heights for Daajing Giids are provided in Table 2-5 above and for Langara Point are provided in Table 2-8 below.

Table 2-8. Tidal heights at the Langara Point reference port.

Tidal Height	Langara Point (m, CGVD2013)
HHWLT	2.6
HHWMT	1.8
MWL	0.2
LLWMT	-1.6
LLWLT	-2.6

Notes: 1. The local conversion from Canadian geodetic vertical datum of 2013 (CGVD2013) to chart datum (CD) at Langara Point is +2.61 m as per CHS benchmark no. 10-1973.

3 WIND REGIME

Winds blowing over water generate waves by transferring energy to the water surface through friction. It is therefore necessary to accurately characterize offshore winds to reliably estimate the wave climate in the study area. NHC analyzed historical winds to understand the nature of the wind regime that can affect the shoreline along the northern and eastern coasts of Graham Island. The areas of interest for this study are mainly exposed to waves coming from the general directional sectors shown in Figure 3-1 and listed as follows:

- Dixon Entrance westerly (DEW) sector
- Dixon Entrance easterly (DEE) sector
- Hecate Strait northerly (HSN) sector
- Hecate Strait southerly (HSS) sector

Notes: DEE – Dixon Entrance east; DEW – Dixon Entrance west; HSN – Hecate Strait north; HSS – Hecate Strait South

Figure 3-1. General open-water exposure of the project's study areas.

3.1 Meteorological Stations

NHC assessed historical wind records from several meteorological stations to identify the stations most appropriate to represent the five study areas. Based on the duration of record, exposure, and confidence in data quality, the most appropriate wind-measuring stations were chosen to represent each overwater sector. For Dixon Entrance, Langara Island (ECCC station no. 1054503) was selected to represent westerly winds, and Rose Spit (ECCC no. 1056869) was selected to represent easterly winds. In northern Hecate Strait, Sandspit Airport (ECCC station no. 1057051) was selected to represent southeasterly winds, and Bonilla Island (ECCC station no. 1060R0K) was selected to represent northerly winds. The location of these stations is shown in Figure 1-3, and associated details are provided in Table 3-1. Between 1972 and 2001, winds at Langara Island were recorded every 3 hours and during the daytime only.

Table 3-1. ECCC meteorological stations representative of winds in Dixon Entrance and northern Hecate Strait.

Station Name	Representative Area	Year Start	Year End	Data Missing
Langara Island	Dixon Entrance	1972	Present	2001 – 2004
Rose Spit	Dixon Entrance	1994	Present	1994 – 2004
Sandspit Airport	Hecate Strait	1953	Present	1999 – 2001, 2004 – 2010
Bonilla Island	Hecate Strait	1994	Present	1994 – 2004[1]

For the Sandspit Airport, an unexpectedly high concentration of severe storms was recorded from 1954 to 1957. Upon further investigation, it was found that a Dines-type **anemometer** was used during this period before it was replaced with a more reliable U2A-type anemometer, which is the same type used at the other stations listed. As a result, the data recorded during this period were omitted from the analysis to achieve greater consistency.

NHC also examined the winds recorded at the wave buoys in Dixon Entrance and Hecate Strait, shown in Figure 1-3. Although these buoys are technically better located to measure winds as they are far from the influence of land topography, the motion of the buoys under the passing waves, in conjunction with the relatively low height of the instrument in relation to the wave heights, reduces the reliability of the measurements. Nevertheless, such measurements are considered relevant for verification purposes.

3.2 Wind Adjustments

Winds measured at meteorological stations can be affected by various factors, which sometimes need to be accounted for to reflect the offshore conditions that generate waves. This section presents the adjustments NHC made to the measured winds.

When developing standard methodologies for estimating wave climate from wind measurements, wind speed is standardized to a height of 10 m above the local ground or water surface. Because wind speed

can vary considerably depending on the elevation at which it is being measured, NHC adjusted the measurements of the anemometers to the 10 m standard elevation above local ground or sea level, as applicable, by using the procedure presented in the *Coastal Engineering Manual* by the US Army Corps of Engineers (USACE, 2002).

NHC estimated the elevation of anemometers at the ECCC meteorological stations based on published information in conjunction with publicly available photographs. Wind speed at the buoys was adjusted considering an anemometer height of 5 m above the water surface. Since wind speed measured at land-based stations can also be affected by friction with vegetation and topography (e.g., land features), NHC also made adjustments to account for these effects. Missing data within gaps less than three hours were interpolated using linear interpolation.

3.3 Wind Analysis

This section presents the results of NHC's wind analysis for Dixon Entrance, Masset Inlet, and Hecate Strait.

Storm systems in this region of the northeast Pacific experience seasonally opposed winds that are strongest in the winter months. According to Walker and Barrie (2006), the **Aleutian Low** develops and intensifies, causing a counter-clockwise circulation of low-altitude winds. From October through April, this low-pressure system brings southerly and southeasterly winds up Hecate Strait and over Haida Gwaii in general. With the arrival of spring, the Aleutian Low declines and retreats to the northwest, while the **North Pacific High** expands and intensifies, which shifts the dominant southeasterly winds to a northwesterly dominant direction in the summer.

3.3.1 Dixon Entrance

Wind roses are diagrams used to show wind magnitude, direction, and frequency. Each stem characterizes the wind coming from the direction in which it expands outwards; the individual length of the coloured segments along a stem represents the frequency of the wind within a specific speed range.

Figure 3-2 (left) presents wind roses for the meteorological stations at Langara Island (left panel) and Rose Spit (right panel). The station at Langara Island is located on the northwest shoreline of the island and is exposed to westerly winds coming from the Pacific Ocean; this station was thus initially selected to describe the overwater winds inside Dixon Entrance coming from that direction (the DEW sector). Moderate (e.g., > 10 metres per second [m/s]), generally westerly winds are spread from south to north, with a distinct focus for winds coming from the west. Overall, the wind rose shows most of the recorded winds are relatively mild (e.g., < 10 m/s), and strong winds (e.g., > 17.5 m/s or **gale force**) are rare; for this reason, the length of the stem segments representing such wind speeds is too short to be detected visually in the wind rose.

The Rose Spit meteorological station (Figure 3-2, right) is well exposed to winds coming from all directions, although winds from the southeast prevail, with westerly winds being the second most frequent. Although less frequent, strong winds from the east still occur and can generate waves over the

open-water **fetches** leading to the exposed shorelines of the Village of Masset. Rose Spit was initially considered to characterize the overwater winds coming the DEE sector inside Dixon Entrance.

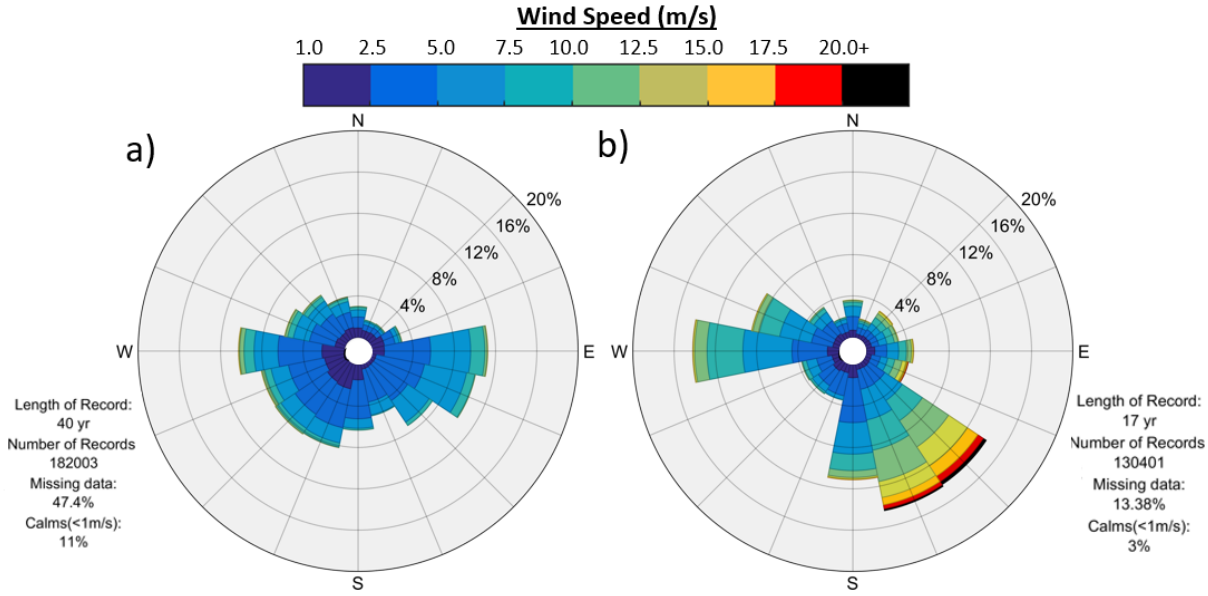

Figure 3-2. Wind roses for wind at a) Langara Island and b) Rose Spit.

NHC further explored the incidence of strong winds in Dixon Entrance by examining the winds measured at the west and central Dixon Entrance wave buoys (Figure 3-3). As noted previously, wind measurement may be affected by the motion of buoys in comparison to measuring wind at a land-based station, but these measurements are still considered useful for providing insight into the milder winds recorded at Langara Island.

Moderate westerly winds occur from all directions in the open ocean, as shown in the left wind rose in Figure 3-3, which is situated at the west Dixon Entrance buoy; a greater frequency of winds in this area occur from the south-southeast and northwest. Relatively stronger winds are focused from the southeast and west-northwest at the central Dixon Entrance buoy (Figure 3-3, right). Generally, both buoys show a higher frequency of stronger winds in comparison to Langara Island (Figure 3-2, left). Furthermore, the easterly winds measured at the central Dixon Entrance buoy are more frequent and stronger than the easterly winds measured at Rose Spit.

Based on these observations, even though measurements at a land-based station are generally more reliable, the study team ultimately considered the winds measured at the central Dixon Entrance buoy to represent the overwater winds in Dixon Entrance.

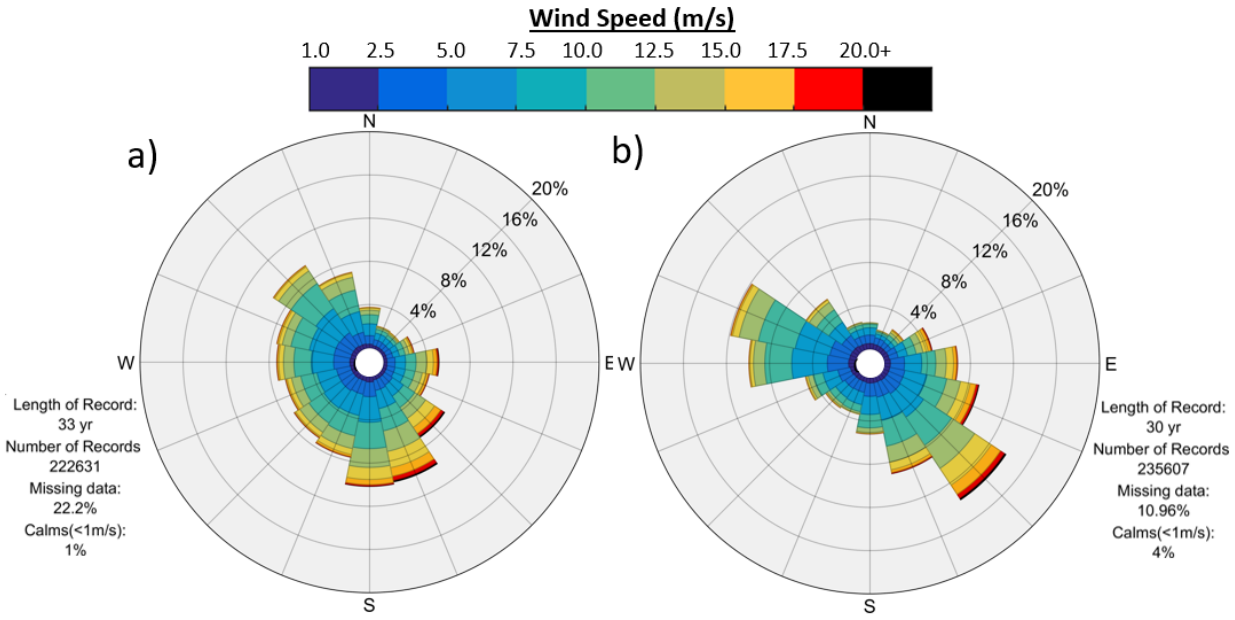

Figure 3-3. Wind roses for wind at wave buoys in a) west Dixon Entrance and b) central Dixon Entrance.

The five most severe storms were identified from each of the two prevailing sectors in Dixon Entrance based on both wind speed and duration. These storms are listed in Table 3-2 and Table 3-3 for the westerly (DEW) and easterly (DEE) sectors, respectively.

Table 3-2. Top five most severe westerly storms measured in Dixon Entrance.

Date (YYYY/MM/DD)	Peak Wind Speed (m/s)	Peak Wind Direction (°T)*	Consecutive Hours Above Gale Force	Location Measured
2014/11/06	27.1	245	6	Central Dixon
2010/10/10	26.1	290	2	Langara Island
2012/01/24	24.1	265	4	Central Dixon
2000/03/21	23.3	230	9	Langara Island
2012/01/25	22.9	260	4	Central Dixon

Note: * °T refers to the direction in degrees with respect to **true north**, measured clockwise.

Table 3-3. Top five most severe easterly storms measured in Dixon Entrance.

Date (YYYY/MM/DD)	Peak Wind Speed (m/s)	Peak Wind Direction (°T)*	Consecutive Hours Above Gale Force	Location Measured
2015/01/04	26.7	70	24	Central Dixon
1999/10/25	26.5	123	10	Central Dixon
2018/10/24	24.2	119	13	Central Dixon
2001/10/26	22.4	50	7	Central Dixon
2006/12/10	22.0	120	13	Rose Spit

Note: °T refers to the direction in degrees with respect to true north, measured clockwise.

NHC conducted a **peak-over-threshold analysis** for westerly and easterly winds at the central Dixon Entrance buoy, using a gale force wind of 17.5 m/s as the threshold. The team also conducted an **extreme value frequency analysis** on the results to estimate the wind speed associated with various AEPs (Table 3-4). NHC then performed the same analysis on the measurements at the respective ECCC meteorological stations, which resulted in similar wind speeds for AEPs less than 5% (i.e., the less frequent winds), but slightly slower winds for AEPs greater than or equal to 5% (i.e., the more frequent winds).

Table 3-4. Wind speed of varying AEP for Dixon Entrance.

AEP	Wind Speed (m/s)	
	Westerly Sector (Central Dixon Entrance Buoy)	Easterly Sector (Central Dixon Entrance Buoy)
0.5%	27.9	27.1
1%	26.9	26.4
2%	25.9	25.7
5%	24.6	24.8
20%	22.6	23.4
Annual	20.0	21.7

3.3.2 Masset Inlet

No long-term wind records are available for Masset Inlet, and sources of wind information for the area are limited. Nevertheless, such information remains useful for developing a general understanding of the winds in that part of Haida Gwaii. The available sources of wind data include the following:

- Mean daily observations reported at a buoy operated by the BC Ministry of Forests, Land, Natural Resources Operations & Rural Development[4] (FLNRORD) from 1984 to 1994
- The High-resolution Deterministic Prediction System (HRDPS) weather forecasting model operated by ECCC, from which hourly predictions were collected from 2017 to 2021 on a 2.5 km grid[5]
- ERA5 atmospheric reanalysis model operated by the European Centre for Medium-Range Weather Forecasts (Hersbach et al., 2020); the spatial resolution of the wind data is 0.25° (approximately 30 km) and spans from 1979 to 2020

The wind rose summarizing the main daily observations at the historical FLNRORD buoy is presented in Figure 3-4. The strongest and most frequently occurring winds in Masset Inlet come from the east and southeast, but frequent northwesterly winds also occur. The buoy data are insufficient to draw any meaningful conclusions on wind magnitude, however, since the available observations are shown in mean daily values. Additional background information on data collected from the buoy (e.g., sampling interval, instrumentation, and precise location) was requested from FLNRORD, but such information was

[4] This ministry has undergone many name changes including the most recent in April 2022, which created two new ministries, namely, the Ministry of Forests and the Ministry of Land, Water and Resource Stewardship.

[5] NHC has developed proprietary software to archive and utilize the HRDPS weather model outputs. These include surface winds and pressures on a 2.5 km grid for all of Canada.

not available at the time of the study[6]. Wind direction was reported in 45-degree sectors, which explains the limited number of stems in the wind rose.

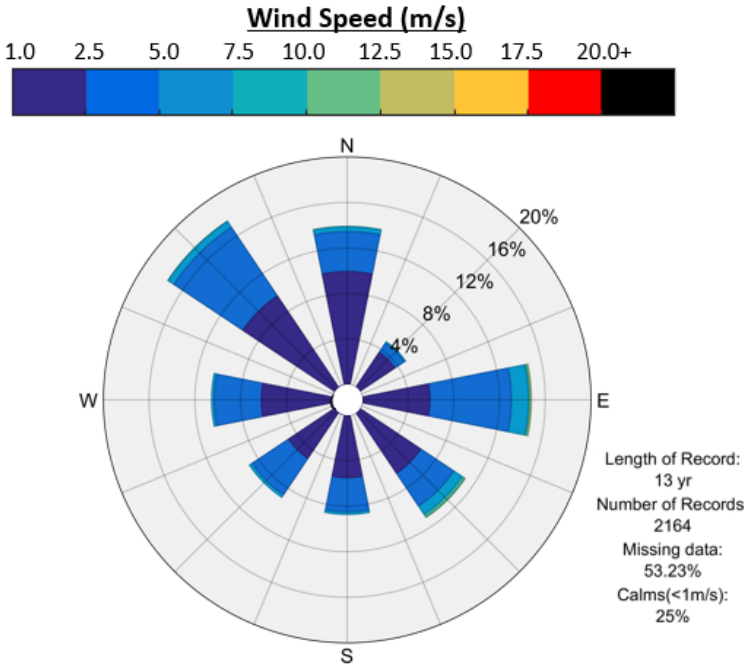

Figure 3-4. Wind roses for mean daily winds reported at historical buoy in Masset Inlet (1982 – 1995).

Figure 3-5 shows wind roses for hourly wind predicted by the HRDPS weather forecasting model (left) and the ERA5 reanalysis model (right). Both datasets suggest that the strongest and most frequent winds in Masset Inlet come from the southeast, which is relatively consistent with the observations made at the historical FLNRORD buoy (Figure 3-4). Winds from other directions are generally distributed, with a slightly higher frequency from the northwest. In addition, the models' wind roses show similarities with the wind rose of the central Dixon Entrance buoy (Figure 3-3, right), although the former shows considerably stronger winds.

The reliability of atmospheric models can vary greatly, especially at the length scale considered for this study, and no adequate field data are available to validate the model predictions. Based on these factors, the winds measured at the central Dixon Entrance buoy are considered representative of the winds blowing in Masset Inlet. Such assumptions err on the conservative side and can be confirmed by field monitoring if required.

[6] FLNRORD, 2021. Request was documented in an email communication between Logan Ashall (lashall@nhcweb.com) and Jasmine Bulbrook (jasmine.bulbrook@gov.bc.ca) on November 02, 2021.

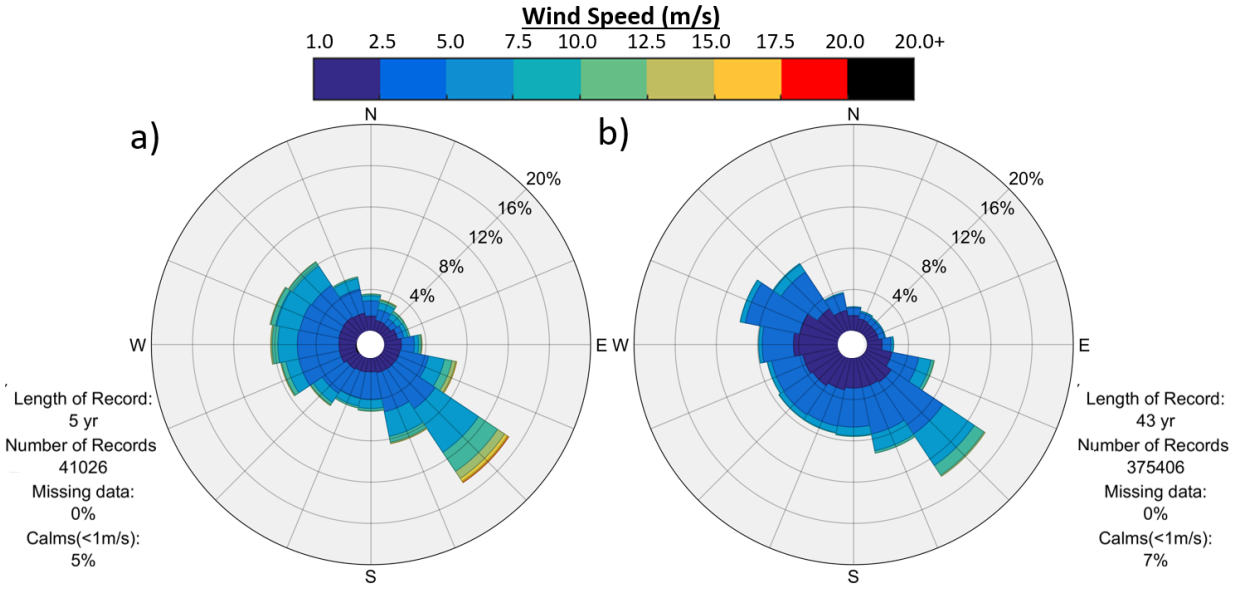

Figure 3-5. Wind roses for hourly wind predicted by a) the HRDPS weather forecasting model for the 2017 – 2021 period and b) the ERA5 reanalysis model for the 1979 – 2020 period.

3.3.3 Hecate Strait

Figure 3-6 shows wind roses for the meteorological stations at Sandspit Airport (left) and Bonilla Island (right). Both stations measure strong and frequent winds from the southeast. In comparison to Bonilla Island, Sandspit Airport shows a relatively small occurrence of northerly winds, although this location experiences more westerly winds. Given its proximity to the study areas and similar exposure to the southeast in comparison to Bonilla Island, Sandspit Airport is considered more representative of the southeasterly winds from the HSS sector.

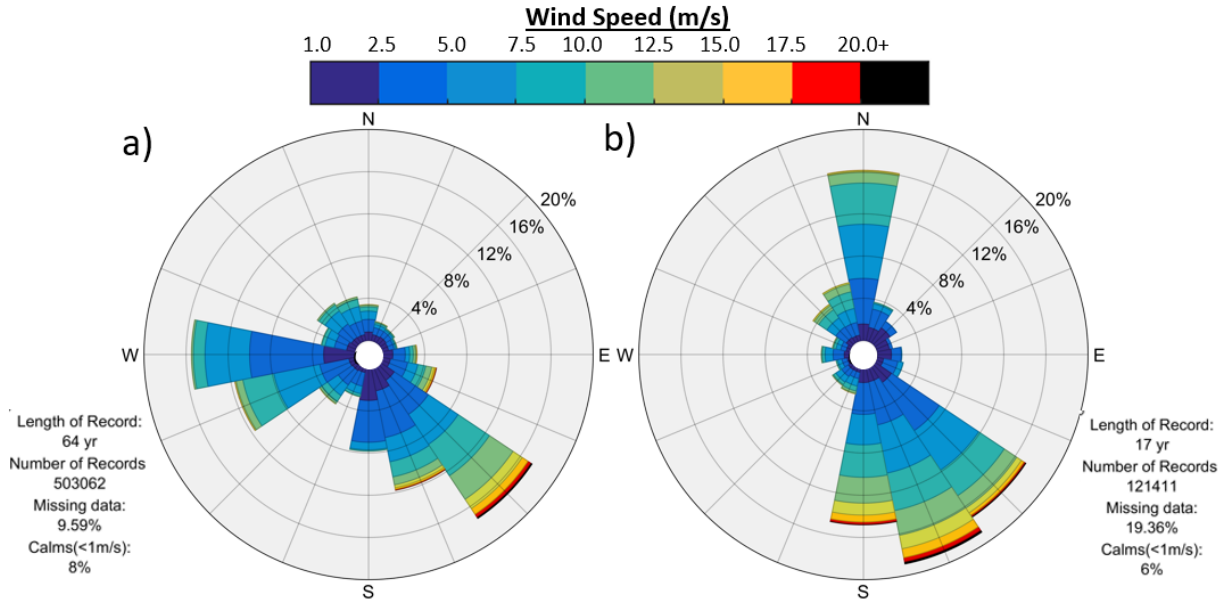

Figure 3-6. Wind roses for wind at a) Sandspit Airport and b) Bonilla Island for their respective period of record.

The winds (and waves) expected to be most detrimental to the community of Sandspit along the western shore of Haida Gwaii come from the northerly sector, more specifically, from the north-northeast. Both roses for Sandspit Airport and Bonilla Island show relatively little occurrence of winds from this direction; therefore, NHC reviewed winds measured at the north Hecate Strait wave buoy, which are presented by the wind rose in Figure 3-7 (left). Winds measured at the south Hecate Strait buoy are also shown for completeness (Figure 3-7, right).

Generally, in comparison to Bonilla Island (Figure 3-6, right), wind conditions at the north Hecate Strait wave buoy (Figure 3-7, left) show a higher frequency of winds from the northwest and a relatively equal frequency of winds from the north-northeast. However, since north-northeast winds appear stronger at the buoy, winds measured at the north Hecate Strait buoy were ultimately considered as representative of the northerly overwater winds (HSN sector) affecting the areas of interest.

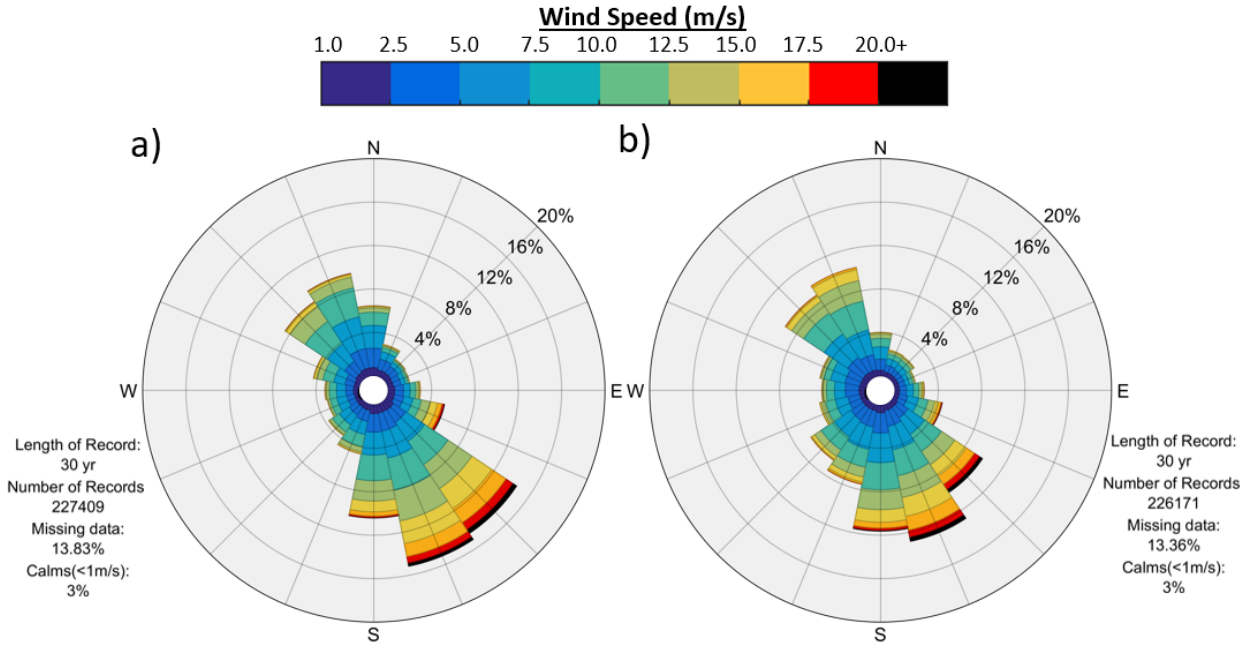

Figure 3-7. Wind roses for wind at wave buoys in a) north Hecate Strait and b) south Hecate Strait for their respective period of record.

The five most severe storms were identified from each of the two prevailing sectors in Hecate Strait based on wind speed and duration. These storms are listed in Table 3-5 and Table 3-6 for the southerly (HSS) and northerly (HSN) sectors, respectively.

Table 3-5. Top five most severe southeasterly storms measured in Hecate Strait.

Date (YYYY/MM/DD)	Peak Wind Speed (m/s)	Peak Wind Direction (°T)	Consecutive Hours Above Gale Force	Location Measured
2012/11/22	28.9	158	7	North Hecate Strait buoy
2006/11/19	28.3	146	8	North Hecate Strait buoy
2010/03/11	28.2	148	26	North Hecate Strait buoy
2018/12/14	27.7	150	17	Sandspit Airport
2007/12/22	27.7	136	20	North Hecate Strait buoy

Note: °T refers to the direction in degrees with respect to true north, measured clockwise.

Table 3-6. Top five most severe northerly storms measured in Hecate Strait.

Date (YYYY/MM/DD)	Peak Wind Speed (m/s)	Peak Wind Direction (°T)*	Consecutive Hours Above Gale Force	Location Measured
2006/03/08	23.4	351	11	North Hecate Strait buoy
2006/04/18	22.2	349	18	North Hecate Strait buoy
2006/02/07	22.1	351	43	North Hecate Strait buoy
2016/12/31	21.0	350	14	Bonilla Island
2009/02/25	19.5	34	11	North Hecate Strait buoy

Note: °T refers to the direction in degrees with respect to true north, measured clockwise.

NHC performed a peak-over-threshold analysis for southerly winds at Sandspit Airport and northerly winds at the north Hecate Strait wave buoy using gale force wind speed of 17.5 m/s as the threshold. The study team then conducted an extreme value frequency analysis on the results to estimate the wind speed associated with various AEPs (Table 3-7). For south-southeasterly winds, the same analysis was performed on the measurements at the north Hecate Strait buoy, resulting in slightly faster winds (e.g., faster by 1 m/s); however, the results for Sandspit Airport are reported due to its longer period of record.

Table 3-7. Wind speed of varying AEP for Hecate Strait.

AEP	Wind Speed (m/s)	
	Southerly Sector (Sandspit Airport)	Northerly Sector (North Hecate Strait Buoy)
0.5%	25.7	30.9
1%	24.6	30.2
2%	23.5	29.5
5%	22.0	28.6
20%	19.7	27.2
Annual	16.8	25.4

4 OFFSHORE WAVE CLIMATE

This section presents the wave information recorded at DFO-operated offshore wave buoys to help characterize the general wave conditions inside Dixon Entrance and Hecate Strait. Such conditions are analyzed further in Appendix C, which presents the wave modelling performed to inform how offshore waves propagate toward the shorelines of the study areas.

Wave buoys considered for the analysis are presented below, followed by wave observations. These observations do not include wave direction; it is important to distinguish the sector where waves originate from when establishing statistics, so NHC conducted additional analysis to infer wave direction from available metocean parameters.

4.1 Wave Buoys

The four wave buoys considered for this study are listed in Table 4-1; buoy locations are shown graphically in Figure 1-3 in relation to Haida Gwaii. Central Dixon Entrance and north Hecate Strait buoys were considered to characterize wave conditions offshore of the study areas, while west Dixon Entrance and south Hecate Strait were mainly used to define boundary conditions for the numerical wave model. Wave modelling was performed to identify flooding hazards at the study areas and is presented in Appendix C.

No wave observations are available for Masset Inlet; associated wave information for that area was derived from wind information alone, in conjunction with numerical modelling.

Table 4-1. Wave buoys located in the study area.

Buoy Name	Station Number	Year Start	Year End	Data Missing
West Dixon Entrance	C46205	1989	2021	2001, 2012, (2018-2020)[1]
Central Dixon Entrance	C46145	1991	2021	2009
North Hecate Strait	C46183	1991	2021	2019[1]
South Hecate Strait	C46185	1991	2021	2014

Notes: 1. A dense concentration of unrealistically large waves for that area (up to H_s = 20 m) were noticed in the available record for those years. Accordingly, the measurements over that period are considered unreliable and NHC removed them from the analysis.

4.2 Wave Observations

Observed wave heights and periods at the central Dixon Entrance and north Hecate Strait buoys are presented below. Since no information is available for wave direction, NHC analyzed **wave steepness** to obtain insight into the nature of the waves. More specifically, the team sought to determine whether the waves consist of a **swell** originating from the open ocean or from locally generated **wind sea**. Furthermore, time series of storms are presented for inferring the general direction of the measured waves, which is discussed specifically in Section 4.3.

4.2.1 Dixon Entrance

This section presents the results of NHC's processing of wave observations in Dixon Entrance, specifically, wave heights, wave period and steepness, and the temporal characteristics of storms in this area.

4.2.1.1 Wave Heights

Figure 4-1 shows the **significant wave height** (H_s) of waves measured at west and central Dixon Entrance buoys over a typical period from 1995 to 2000. Observations show that larger wave events occur more frequently during the winter than during the summer months. Waves in Dixon Entrance are generally smaller in comparison to the open sea. The top five largest wave events measured in central Dixon Entrance are listed in Table 4-2.

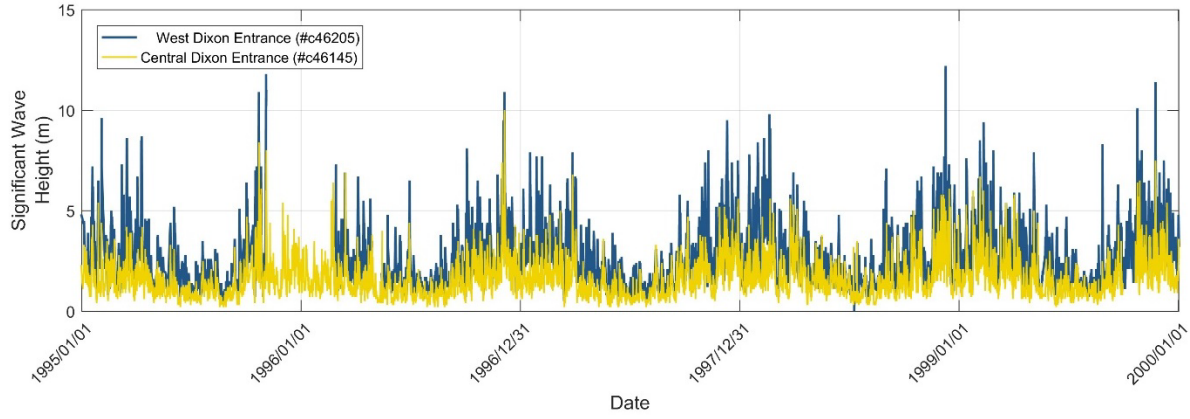

Figure 4-1. Wave buoy observations at west (blue) and central (yellow) Dixon Entrance buoys from 1995 to 2000.

Table 4-2. Top five largest wave events in central Dixon Entrance.

Date (YYYY/MM/DD)	Significant Wave Height (m)	Peak Wave Period (seconds)
1992/12/14	11.3	17.1
2006/12/24	10.9	18.3
1996/12/05	10.0	16.0
2011/11/13	9.3	15.1
1994/11/27	8.5	16.0

4.2.1.2 Wave Period and Steepness

Figure 4-2 shows the **peak wave period** (T_p) associated with various occurrences of wave height in Dixon Entrance. While short periods (e.g., T_p < 9 seconds) are typically associated with relatively smaller waves (e.g., H_s < 6 m), longer periods, which are characteristic of swells, can be associated with both smaller and larger waves.

Measurements of wave heights by DFO-operated buoys are typically grouped into discrete values of peak wave period. This explains the vertical grouping of data points visible in Figure 4 2. There are times, however, when the buoy does not record the peak wave period and thus would need to be derived from wave spectrum parameters. In such instances, the wave heights are provided as per the peak wave period derived by DFO, which explains the group of points for smaller waves with longer period.

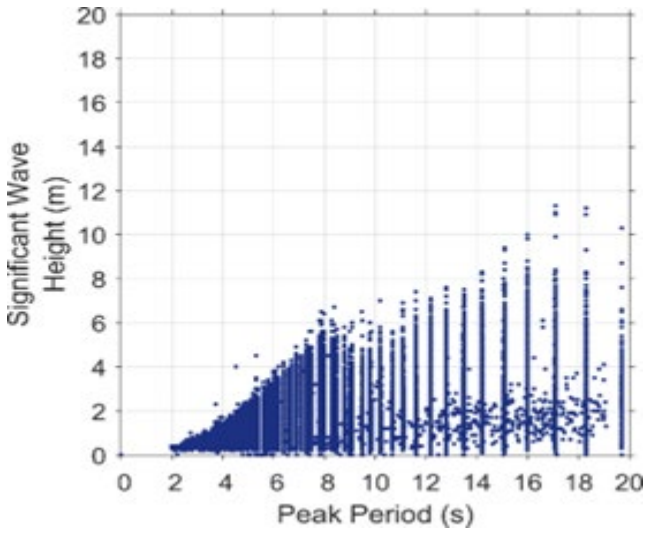

Figure 4-2. Occurrences of wave height and wave periods in central Dixon Entrance.

Wave steepness (s) is defined as the ratio of wave height to wavelength, in which the latter can be related to the wave period. Generally, a wave steepness closer to s = 0.01 indicates a typical swell and a steepness of s = 0.04 to 0.06 indicates a typical wind sea (USACE, 2002). The wave steepness is used to understand the distribution of swell and wind sea inside Dixon Entrance, as shown in Figure 4-3. A **transitional sea** is described as a swell over which locally generated wind waves are superimposed to some degree.

In Dixon Entrance, wind sea occurs less than 10% of the time, and swell occurs more than 40% of the time. For the remaining time, waves correspond to a transitional sea state, albeit a large percentage of transitional sea has a wave steepness between 0.01 and 0.02 and is closer to being a swell. Due to the exposure and orientation of Dixon Entrance to the open sea and its limited fetch to the east, it can be reasonably assumed that the swell propagating in Dixon Entrance comes from the west.

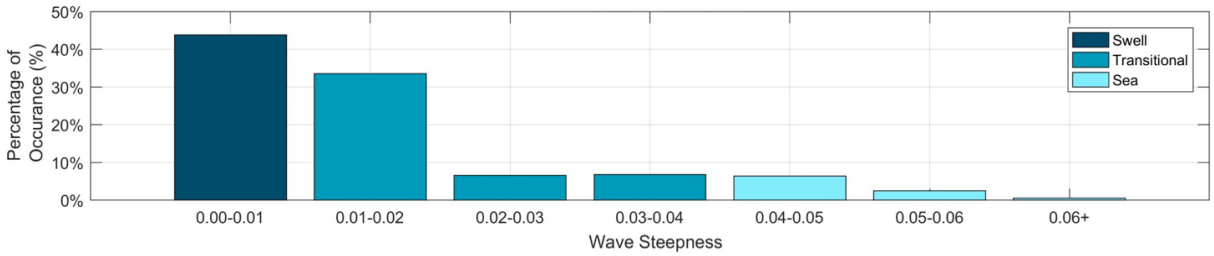

Figure 4-3. Distribution of wave steepness observed in central Dixon Entrance.

4.2.1.3 Storm Temporal Characteristics

NHC analyzed time series of winds and waves measured during storms to understand trends that can be observed during storms and events of considerable wave height, which are referred to here as wave events. This analysis also provides the basis for inferring the general direction of measured waves, which is discussed specifically in Section 4.3.

Time series of wind speed, wind direction, wave height, and wave period for significant wave events in Dixon Entrance are presented and described below. The coinciding observed water level and residual water level (i.e., storm surge) data measured at Langara Island are also presented, when available.

Figure 4-4 shows the time series for a large swell event, which occurred on December 14, 1992. Prior to the event, winds in central Dixon Entrance came from the easterly sector, and the wave measurements suggest a relatively small swell was occurring ($H_s \approx 2$ m and $T_p \approx 12$ sec), likely coming from the open ocean to the west. Winds in central Dixon Entrance remained from the easterly sector for some time, which resulted in a short-lived, predominant wind sea, as shown by the sudden drop in the wave period at approximately 5:00 p.m. on December 12 (down below $T_p = 9$ sec). Winds eventually veered to the westerly sector at approximately 12:00 p.m. on December 13, after which both wave height and wave period considerably increased to a peak of $H_s \approx 11.3$ m with $T_p \approx 17.1$ sec. Such a swell is suspected to have come from the open sea as this gradual increase in wave height was not accompanied by a meaningful increase in wind speed. Such swell conditions were sustained but decreased in intensity.

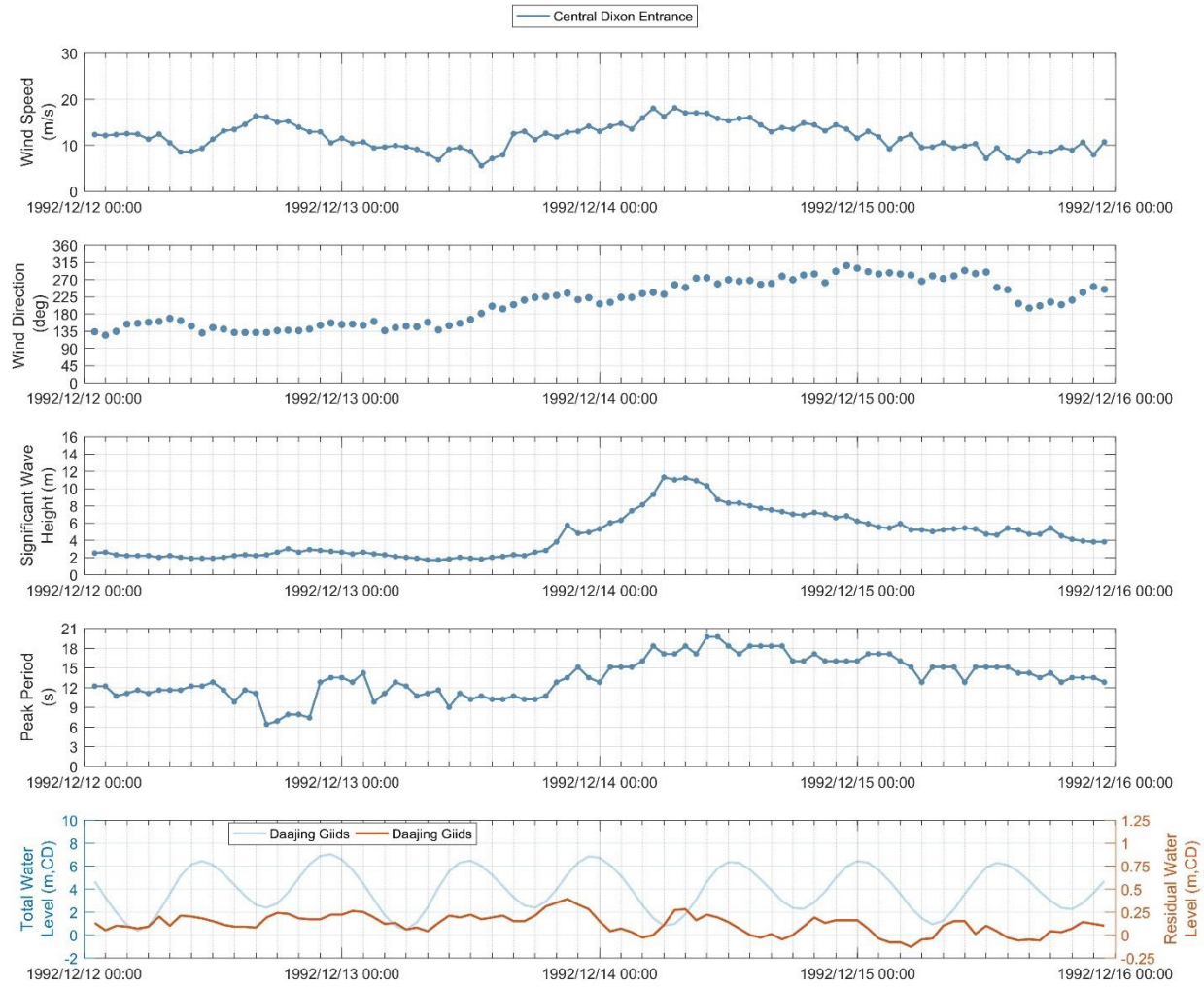

Figure 4-4. Storm of December 14, 1992, and observations in Dixon Entrance – westerly swell. Langara Point water levels are unavailable for this date, so water levels at Daajing Giids are shown instead.

Figure 4-5 show the time series for an easterly storm in Dixon Entrance occurring on November 5, 2014. On the day before the storm, wind speeds were relatively mild (e.g., < 10 m/s) and coming from the westerly sector. Relatively small waves were observed in Dixon Entrance ($H_s \approx 2$ m) with a wave period fluctuating between $T_p = 9$ sec and $T_p = 12$ sec. Winds gradually veered to the easterly sector, passing through the south and considerably increasing in magnitude. This rise was accompanied by an increase in the wave height and, notably, a sudden drop in the wave period, down below $T_p = 9$ sec at approximately 3:00 p.m. on November 5, which indicates the predominance of a wind sea condition. The wind eventually veered back to the west and was accompanied by a decrease in the wave height, but an increase in the wave period was also observed, suggesting the return to a swell or transitional sea condition.

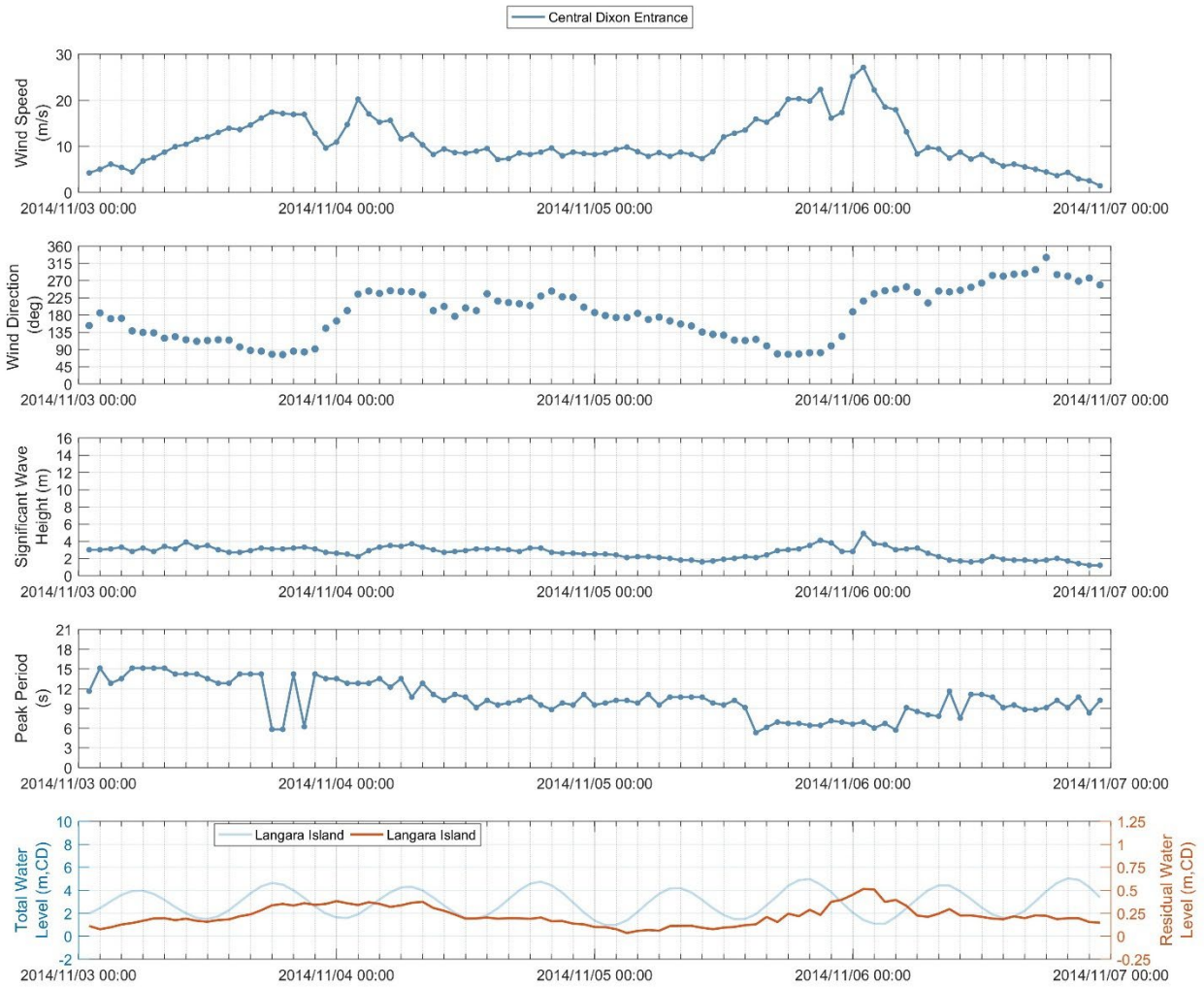

Figure 4-5. Storm of November 5, 2014, and observations in Dixon Entrance – easterly wind sea.

4.2.2 Hecate Strait

This section presents the results of NHC's analysis of wave observations in Hecate Strait, specifically wave heights, wave period and steepness, and the temporal characteristics of storms in this area.

4.2.2.1 Wave Heights

Figure 4-6 shows the significant wave height measured at the north and south Hecate Strait buoys over a typical period from 1995 to 2000. Similar to Dixon Entrance, larger wave events occur more frequently in the winter in comparison to summer months, and waves in southern Hecate Strait tend to be larger, mainly due to the strait's relatively greater exposure to the open ocean. The top five largest wave events measured in northern Hecate Strait are listed in Table 4-1.

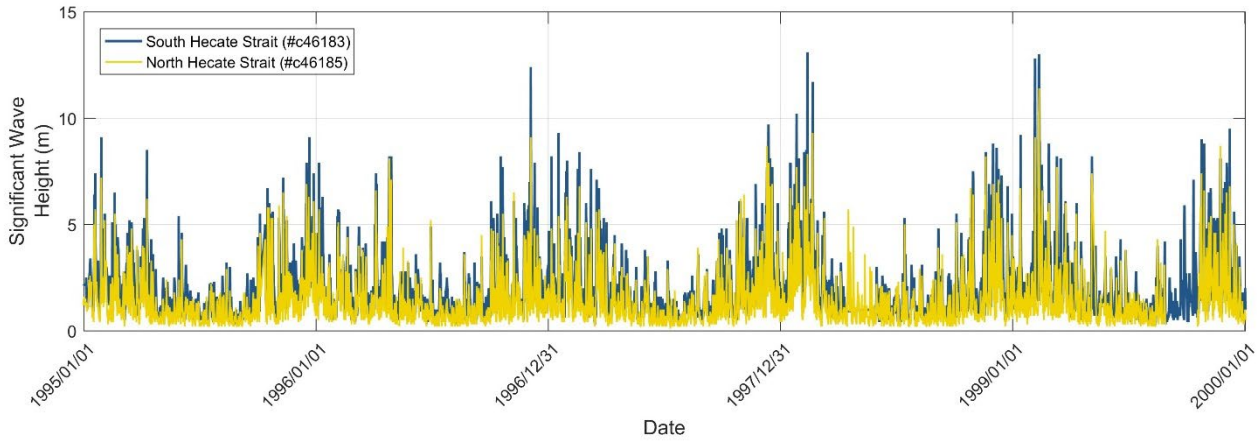

Figure 4-6. Wave buoy observations at north (yellow) and south (blue) Hecate Strait buoys from 1995 to 2000.

Table 4-3. Top five largest wave events in northern Hecate Strait.

Date	Significant Wave Height (m)	Peak Wave Period (seconds)
1992/09/28	13.1	11.6
1999/02/12	11.4	15.1
1991/12/20	10.0	12.8
2010/03/11	9.4	11.1
1998/02/21	9.3	12.8

4.2.2.2 Wave Period and Steepness

The wave period associated with various occurrences of wave height and period in northern Hecate Strait is shown in Figure 4-7. While northern Hecate Strait experiences large waves with similar heights to the ones observed in Dixon Entrance, the wave period associated with these large waves is generally shorter; therefore, the energy associated with these waves is less. The chart also shows that smaller swells (e.g., $H_s < 3$ m) with longer wave periods (e.g., $T_p > 14$ sec) coming from the open ocean can reach the north Hecate Strait buoy; however, the distinction between shorter-period swells and large wind seas isn't as clear in comparison to the waves in Dixon Entrance (Figure 4-2).

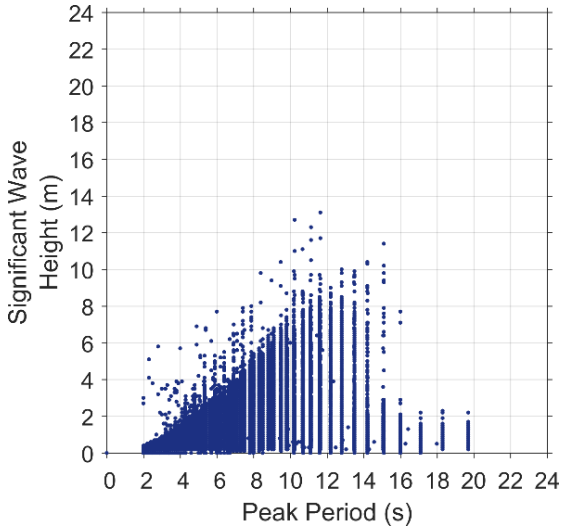

Figure 4-7. Occurrences of wave height and wave period in northern Hecate Strait.

The distribution of the wave steepness observed in northern Hecate Strait is shown in Figure 4-8. Swell occurs under 30% of the time and wind sea approximately 15% of the time. The remaining percentage is attributed to a transitional sea state distributed between distinct swell and distinct wind sea, with a slightly higher concentration trending toward wind sea. This distribution of transitional wave steepness coincides with the occurrences of wave heights and periods observed in Figure 4-7.

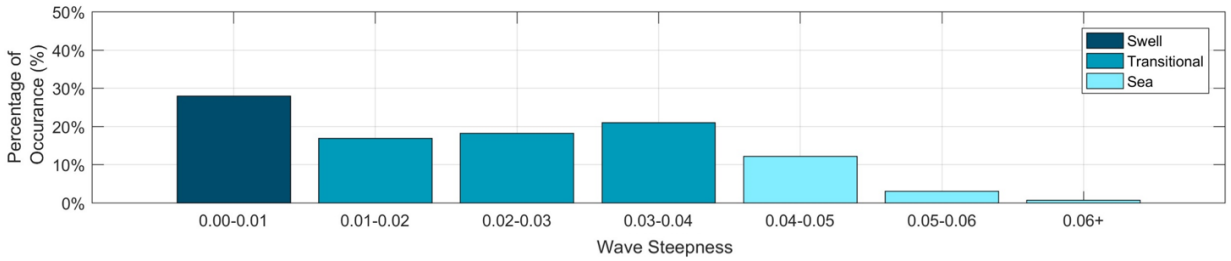

Figure 4-8. Distribution of wave steepness observed in northern Hecate Strait.

4.2.2.3 Storm Temporal Characteristics

The time series of wind speed, wind direction, wave height, and wave period for the southerly storm of December 8, 2014 is presented in Figure 4-9. The coinciding observed water level and the storm surge measured at Daajing Giids are also presented.

Wind speeds before the event were moderate (approximately 10 m/s) from the south. As the storm progressed, the wind slightly shifted to the southeast and wind speeds gradually increased. Moderate to strong winds were sustained over a day before peaking at 22 m/s at approximately 8:00 p.m. on December 8. Following the wind, wave height also gradually increased to H_s = 6 m at the peak of the storm, while the wave period plateaued at 2:00 a.m. on December 9 and fluctuated between T_p = 9 sec and T_p = 12 sec for the remainder of the event.

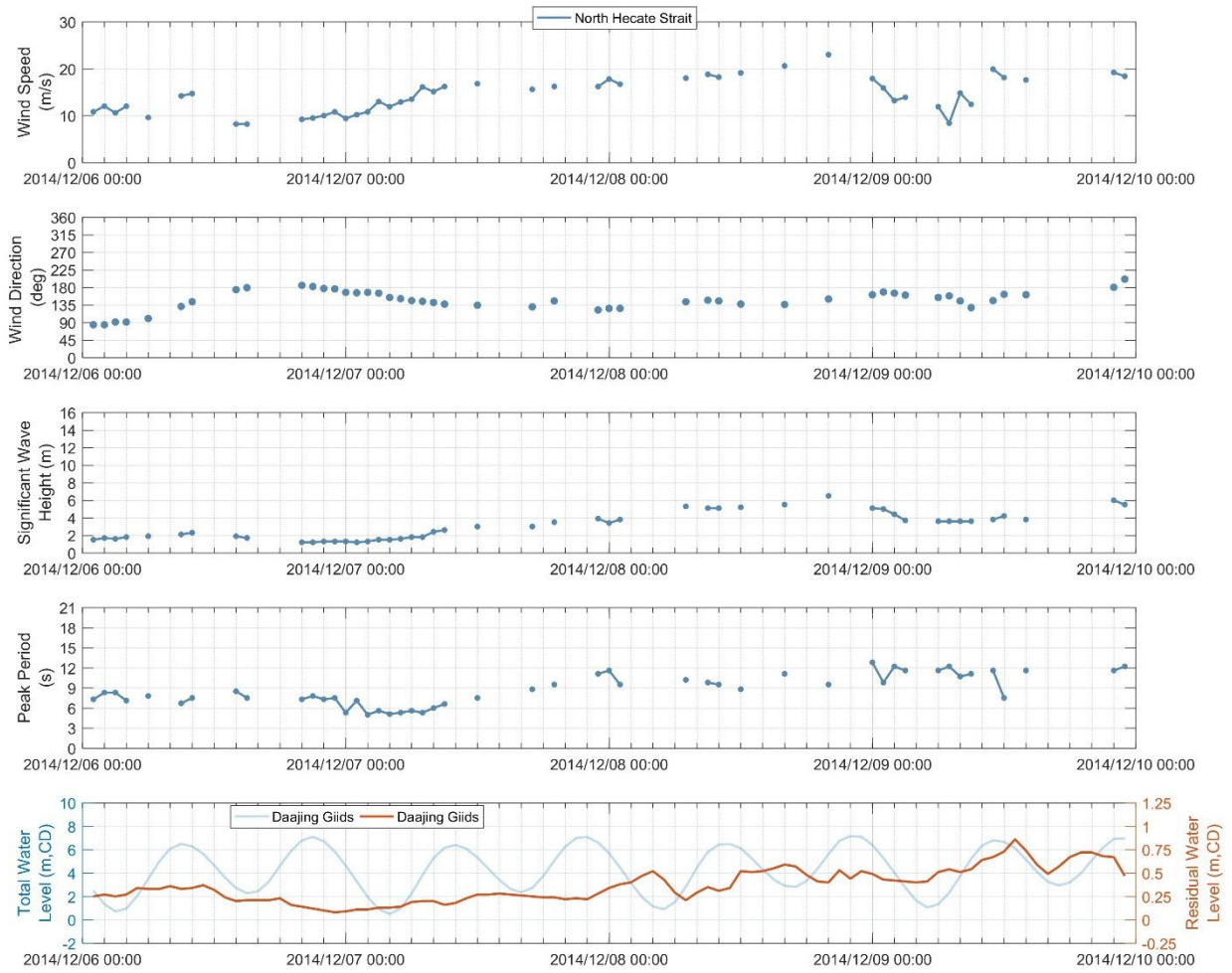

Figure 4-9. Storm of December 8, 2014 and observations in northern Hecate Strait – southerly transitional sea.

Figure 4-10 shows the northerly storm of October 30, 2020. Wind speeds before the event were mild (e.g., < 10 m/s) and from the north, and there were no meaningful waves in the strait. At the onset of the storm, the winds momentarily veered from the north to the east before reversing back to the north for the peak of the storm at 5:00 a.m. on October 30. As the wave height increased, the wave period became longer but remained relatively short ($T_p \approx 8$ sec) in comparison to a longer-period swell. The winds then gradually veered to the west as the winds lost intensity, before essentially becoming calm at approximately 7:00 p.m. on October 30 and being accompanied by a reduction in wave height, thus signalling the end of the event.

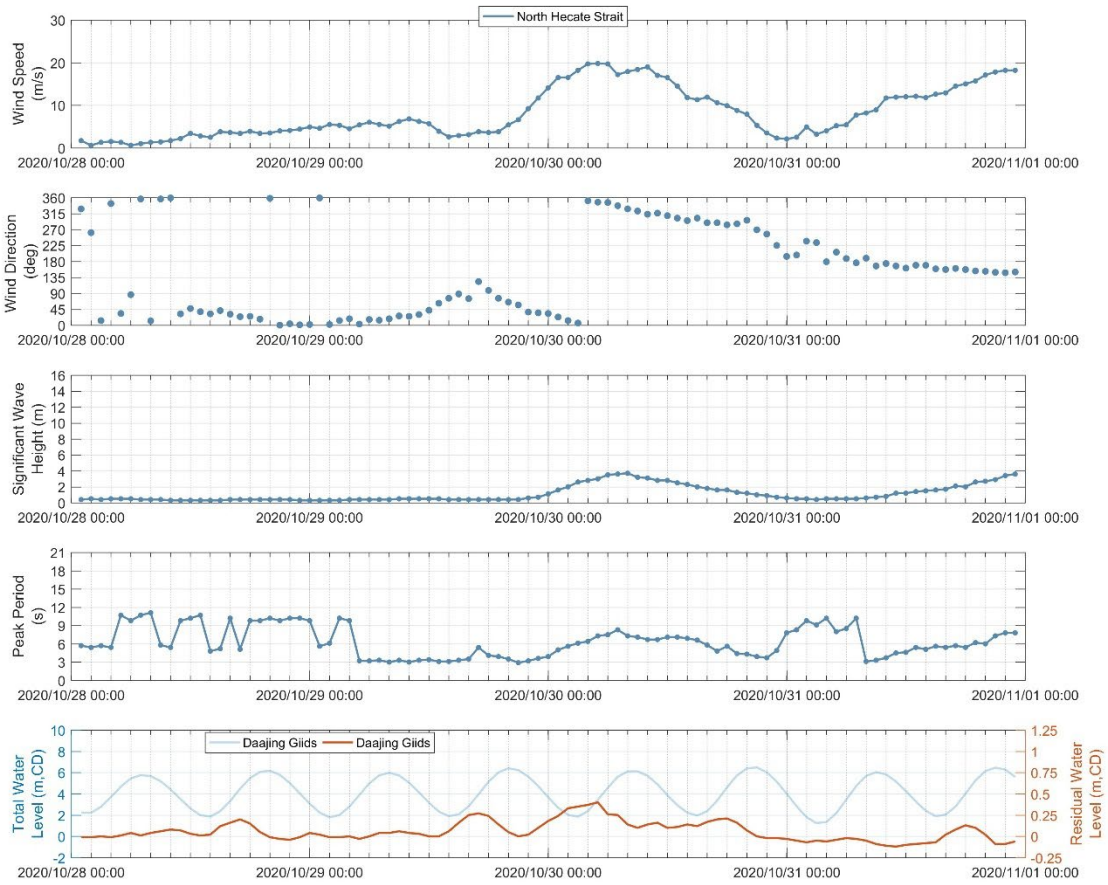

Figure 4-10. Storm of October 30, 2020 and observations in northern Hecate Strait – northerly wind sea.

4.3 Inferred Wave Direction

Given the different orientations of the shorelines within the study area, NHC had to infer a general direction for the wave data to define relevant offshore wave statistics for each overwater sector (Figure 3-1). Such statistics have been computed using a joint probability analysis, as presented in Section 5.

The following sections present the logic followed to infer wave based on available wind and wave observations. In this context, a wave period above T_p = 9.5 seconds is considered a long wave period, and a wind speed over 10 m/s is considered a moderate wind speed. Lastly, a meaningful offshore wave height is considered a wave height greater than H_s = 3 m. These thresholds were used to distinguish the varying metocean conditions that may occur and how they relate to wave direction.

4.3.1 Dixon Entrance

NHC inferred the wave direction in Dixon Entrance based on the direct exposure to the open ocean and the long period of swells that come from that direction. Such a period can easily be compared to the period of easterly, **fetch-limited** waves. Since wind sea can technically come from any direction, the wave direction is considered similar to the wind direction when no swell dominates the measured wave signal. This logic is presented graphically in the flow chart shown in Figure 4-11, which also provides the occurences of each outcome.

The occurrence of swell according to this logic (77% of the time) is in relative agreement with the occurrence of waves with a steepness up to s = 0.02, as shown in Figure 4-3, the latter being a milder wave steepness generally associated with swells.

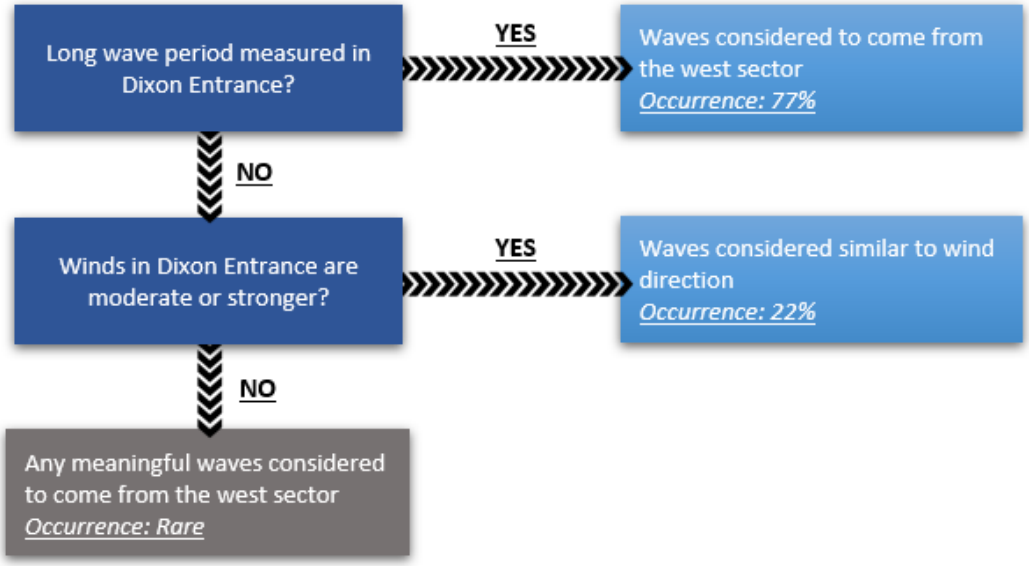

Figure 4-11. Logic used to infer wave direction in Dixon Entrance.

4.3.2 Hecate Strait

In comparison to Dixon Entrance, deducing wave direction in Hecate Strait is complicated by the lack of distinction between shorter-period swells and large wind seas, as indicated by the occurrences of wave height and period shown in Figure 4-7**.** This lack of distinction corresponds with the frequent occurrence of transitional seas (Figure 4-8). The deduction of wave direction is therefore primarily leveraged on the fetch-limited condition of northerly waves and associated generally shorter wave periods. The logic established to infer wave direction in Hecate Strait is presented graphically in the flow chart shown in Figure 4-12, which also provides the occurences of each outcome.

The frequency of swell according to this logic (49% of the time) is in relative agreement with the occurrence of waves with a steepness up to s = 0.02, as shown in Figure 4-8. Using the same reasoning, NHC confirmed that the frequncy of northerly waves (16%) is in relative agreement with the occurrence

of wind sea; the team also determined the frequency of events for which wave direction is assigned, mainly based on wind direction (31%), which is in relative agreement with the occurrence of transitional sea.

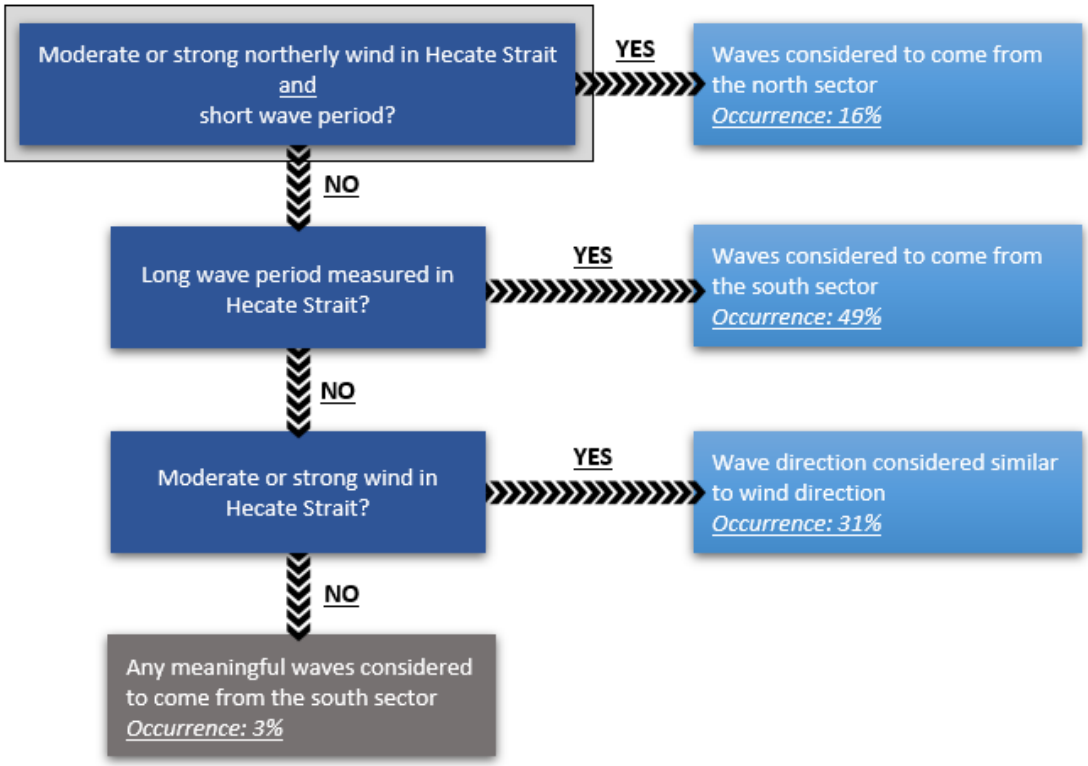

Figure 4-12. Logic used to deduce wave direction in Hecate Strait.

5 JOINT PROBABILITY ANALYSIS

This section presents the results of the probability analysis conducted by NHC to establish the offshore conditions used to estimate coastal flood hazards. First, justification for the analysis is provided, followed by a description of the statistical approach used to conduct the analysis. This section also provides details on the data that were preliminarily processed to support and facilitate the analysis and includes a description of the statistical modelling approach employed. Finally, a summary is presented on the results using joint probability curves.

5.1 Justification

In a coastal environment, static water level and wave height are both factors in the damage that can be inflicted on a coastline. The extent of damage may vary, depending on combinations of these two oceanographic parameters. A smaller wave height combined with a higher water level may be more hazardous than a larger wave height combined with a lower water level, or vice versa depending on local foreshore and backshore characteristics. For this reason, hazards should be assessed against various combinations of water levels and wave heights to establish which combination results in the most adverse conditions at a particular shoreline. NHC used numerical wave modelling to evaluate various combinations of equal exceedance probability, as presented in Appendix C.

5.2 Statistical Approach

Total water level corresponds to the observed water level measured by tide gauges and is derived by adding tide level to storm surge. These two independent components are the product of distinct independent astronomical and atmospheric forcing mechanisms. When conducting an extreme value frequency analysis, storm surge is assessed as a random variable, while tide level is a deterministic variable because it can be accurately predicted.

While storm surge is a random physical phenomenon and better suited for statistical analysis when isolated, a tide level would need to be assigned separately when assessing coastal flood hazards; selecting a tide level for the analysis would then require additional justification and assessment. Alternatively, when tide is added to storm surge to determine the total water level, one variable intrinsically captures the probability that the storm surge and waves coincide with higher tide. NHC opted for this approach to assess coastal storm flood hazards in Haida Gwaii.

NHC used the statistical ‘R’ software package TEXMEX (Threshold Exceedances and Multivariate Extremes) for this study to develop joint probability curves of wave height and total water level. This statistical modelling software is based on the multivariate extreme value models described in Heffernan and Tawn (2004). The application of such statistical models, referred to as model fitting, consists of the following general steps:

1. Pre-process data to enable resampling of the records of observations to a preferable time interval, and include classification based on the overwater sector (e.g., direction).
2. Select a threshold to define which values to include in the extreme value analysis, expressed as a **percentile**.
3. Separately fit the selected data to a threshold exceedance model based on the methodology of Heffernan and Tawn (2004) for each variable (i.e., wave height and total water level).
4. Generate a larger synthetic dataset using the **Monte Carlo method** to create and allow for empirical calculation of low-probability combinations.
5. Calculate the joint probability curves for the AEPs of interest.

The results obtained when following these steps are presented in the subsections below.

5.3 Data Pre-Processing

Observation records were first classified based on wave direction, and joint probability curves were developed for each overwater sector (Figure 3-1). Records were then resampled from an hourly basis to daily maxima. In the process of directly investigating the hourly data, the team identified several advantages in the process of deriving daily maximum resampling values:

- Increase in the correlation between the two variables by decreasing the potential for desynchronization of the maximum wave height and water level during a storm.
- Decrease in the potential for including multiple observations from the same storm.
- Decrease the computational time required to perform calculations.

After resampling, NHC determined a threshold for selecting the data to include in the statistical analysis. Since the objective of statistical analysis is to define combinations of lower probability, one goal for defining the threshold is to preserve the majority of higher-value data. However, this goal needs to be balanced with the need to include enough data to maintain a correlation between the two variables. Since results are influenced by the choice of threshold, NHC explored several options to balance these goals and decided to use the ninetieth percentile value as the threshold for each variable.

5.4 Statistical Modelling

After processing the observation data, NHC fitted the conditional multivariate extreme value model used by Heffernan and Tawn (2004) to each variable, obtaining a two-dimensional, generalized **Pareto distribution** for each variable. The team used the resulting distributions to generate synthetically larger datasets by applying Monte Carlo methods, which enable empirical calculation of low-probability combinations of the two variables. NHC then converted statistical modelling results from a daily exceedance probability to an AEP (i.e., return period).

5.5 Joint Probability Curves

NHC calculated joint probability curves for annual exceedance probabilities of 10%, 5%, 2%, 1%, and 0.05% for Dixon Entrance and Hecate Strait. These curves are presented in the following subsections.

5.5.1 Dixon Entrance

Figure 5-1 shows the joint probability curves derived for the westerly sector of Dixon Entrance. The results show that for each curve representing combinations of equal probabilities, wave height gradually reduces as the water level increases. For combinations of equal probability, this finding indicates that varying water level values will have considerably different wave height values.

Figure 5-2 shows the joint probability curves for the easterly sector of Dixon Entrance. In comparison to the westerly sectors, the results of our analysis show a lower reduction in wave height as the water level increases, until a point is reached when the wave height drops abruptly. For combinations of equal probability, this finding indicates that varying values of water level are associated with relatively similar values of wave height.

For each curve, the value of the variable when the other variable is at a zero value on the charts independently corresponds with the AEP of that variable. The AEPs of each separate variable are presented in Table 5-1.

Table 5-1. Single-variable AEPs of offshore significant wave height in Dixon Entrance and total water level at Langara Island.

AEP	Dixon Entrance Westerly Sector		Dixon Entrance Easterly Sector	
	Significant Wave Height (m)	Total Water Level (m, CD)	Significant Wave Height (m)	Total Water Level (m, CD)
0.5%	10.30	5.62	7.11	5.71
1%	9.71	5.58	6.89	5.69
2%	9.26	5.54	6.68	5.64
5%	8.44	5.49	6.36	5.59
10%	7.83	5.44	6.09	5.54

Note: CD – chart datum

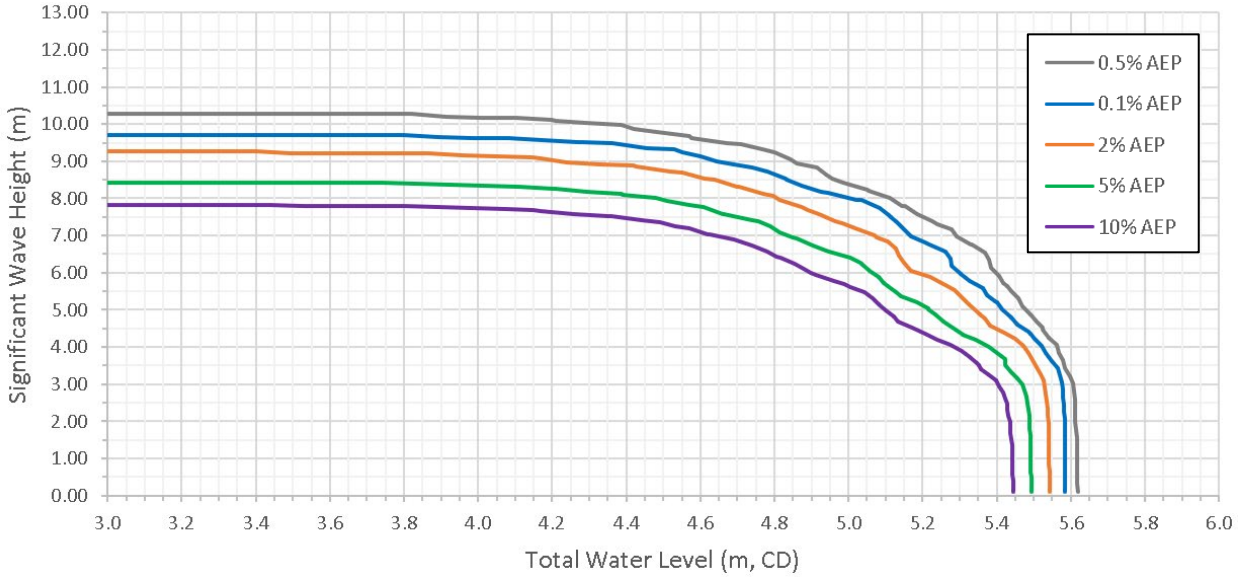

Figure 5-1. Joint probability curves for combinations of total water level and waves from the Dixon Entrance westerly sector.

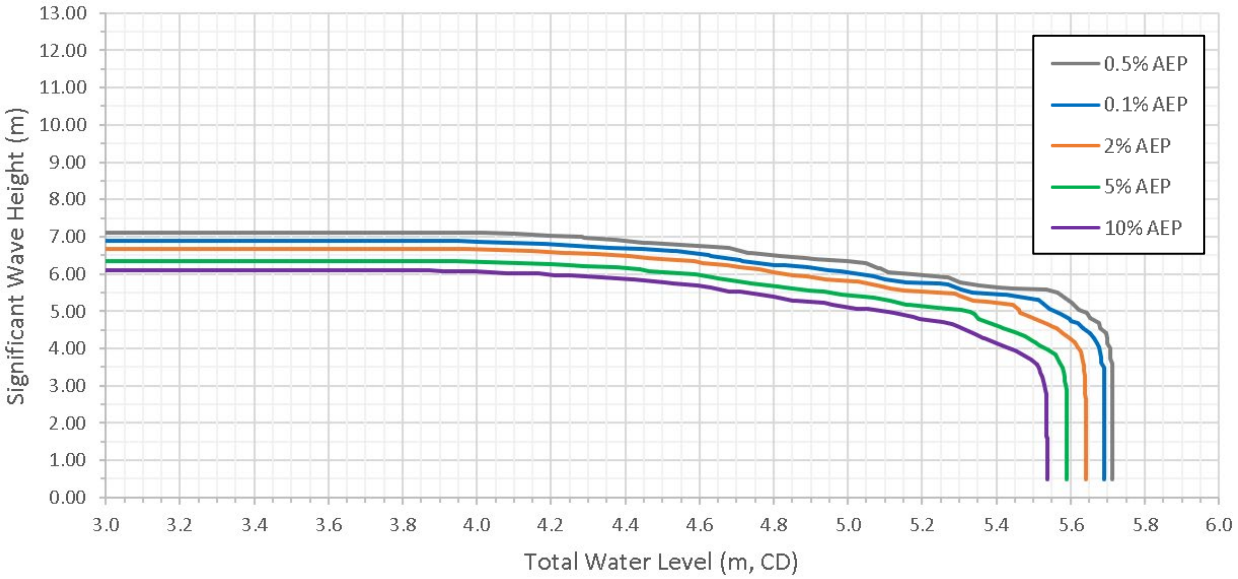

Figure 5-2. Joint probability curves for combinations of total water level and waves from the Dixon Entrance easterly sector.

5.5.2 Hecate Strait

Figure 5-3 show joint probability curves for the northerly sector of Hecate Strait. The curves exhibit a small reduction in wave height as water level increases, up until wave height drops abruptly, similar to the results derived for the Dixon Entrance easterly sector. Figure 5-4 shows the joint probability curves for the southerly sector of Hecate Strait. Similar to the Dixon Entrance westerly sector, the curves exhibit a relatively more gradual rate of reduction in wave height as water level increases.

Table 5-2.presents the AEPs of each variable when considered independently.

Table 5-2. Single-variable AEPs of offshore significant wave height in Hecate Strait and total water level at Daajing Giids.

AEP	Hecate Strait Northerly Sector		Hecate Strait Southerly Sector	
	Significant Wave Height (m)	Total Water Level (m, CD)	Significant Wave Height (m)	Total Water Level (m, CD)
0.5%	5.03	7.67	12.22	7.78
1%	4.85	7.66	11.76	7.77
2%	4.72	7.65	11.41	7.76
5%	4.47	7.63	10.91	7.74
10%	4.22	7.60	10.41	7.71

Note: CD – chart datum

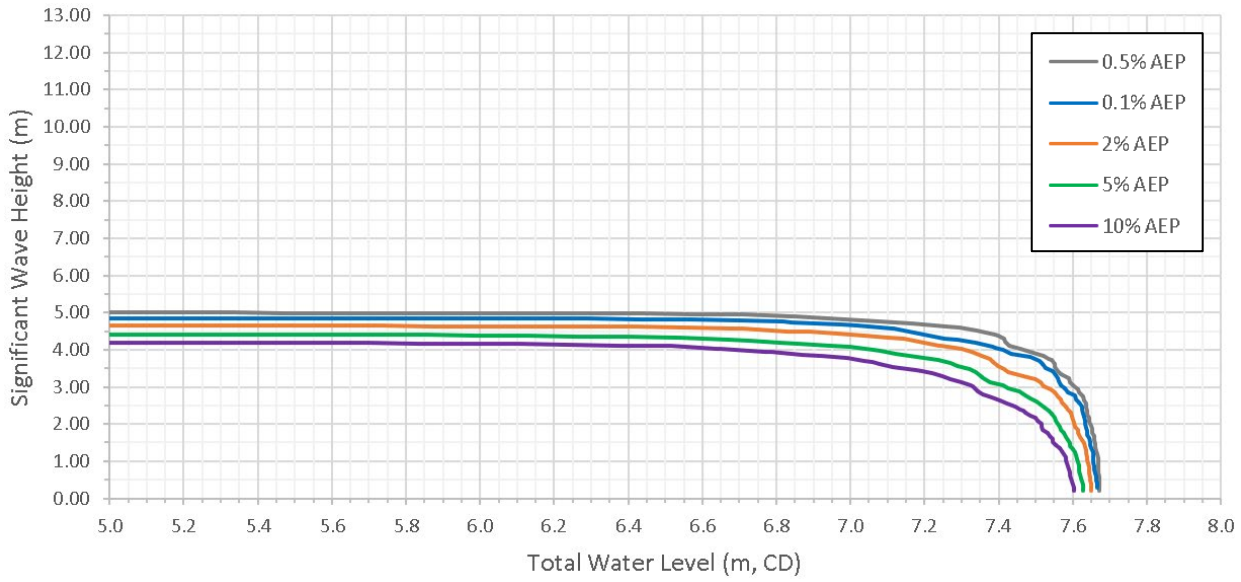

Figure 5-3. Joint probability curves for combinations of total water level and waves from the Hecate Strait northerly sector.

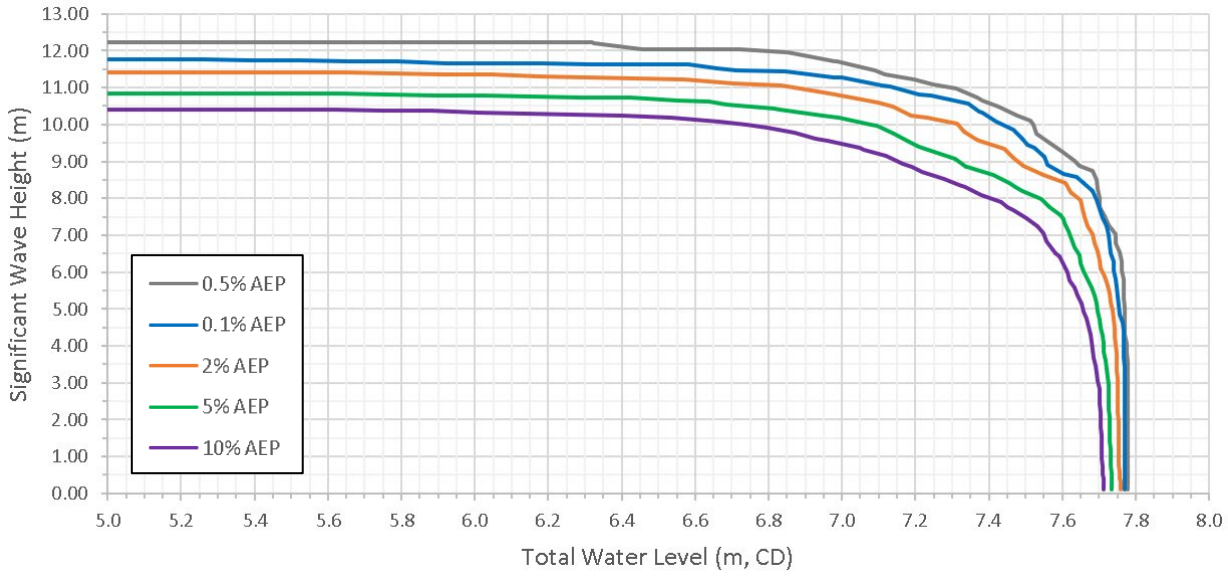

Figure 5-4. Joint probability curves for combinations of total water level and waves from the Hecate Strait southerly sector.

6 SUMMARY

This report summarizes the technical details of the metocean analysis performed to understand the governing conditions offshore of Haida Gwaii. Our detailed assessment of these conditions produced robust, reliable results that can serve as a foundation to support other components of the broader study. The main topics covered in this report are summarized as follows:

1. Haida Gwaii is surrounded by several water bodies that can exhibit varying sea conditions. Water bodies were further divided according to identified areas of interest into the following overwater sectors:
    - Dixon Entrance westerly sector
    - Dixon Entrance easterly sector
    - Hecate Strait northerly sector
    - Hecate Strait southerly sector
2. NHC collected, process, and analyzed historical records from multiple measuring stations to understand the wind regime and wave climate in Dixon Entrance and Hecate Strait. Our team also identified offshore design criteria for consideration in the subsequent assessment of coastal flood hazard along the shoreline.
3. At Langara Point, the tidal range is 5.2 m. in comparison to 7.7 m at Daajing Giids in Skidegate Inlet. The length, width, and relatively shallow depth of Masset Sound directly affects tide propagation, so the tidal range in Masset Sound is smaller than it is in McIntyre Bay. Both the tidal range and the height of high tides further reduces with distance away from McIntyre Bay toward Masset Inlet; the tidal range at Port Clements and Juskatla is 3.0 m and 1.9 m, respectively.
4. The data from measuring stations show that the predominant winds are from the southeast in both Dixon Entrance and Hecate Strait, although strong winds (e.g., > 17.5 m/s or gale force) are more frequent in Hecate Strait in comparison to Dixon Entrance. Strong westerly winds can occur in Dixon Entrance, and strong northerly winds can also occur in Hecate Strait, but will be less frequent.
5. Masset Inlet is classified as its own water body, since it is isolated from open ocean waves although influenced by tides, storm surges, and ocean tsunamis. Waves in Masset Inlet are generated by local winds.
6. Wave measurements available for the study area include wave height and wave period, but not wave direction. Since it is important to distinguish where the sector waves originate from to establish statistics, the team conducted additional analysis to infer wave direction from available metocean parameters.
7. A joint probability analysis was performed to establish design combinations of coinciding water levels and offshore wave conditions, ensuring the conservative use of combinations that are the most adverse at each of the project's areas of interest. NHC evaluated various combinations of equal exceedance probability by conducting wave modelling, and the results of this assessment are presented in Appendix C.

7 REFERENCES

Canadian Hydrographic Service (2022). *Canadian Tide and Current Tables – Queen Charlotte Sound to Dixon Entrance (Volume 7)*. Fisheries and Oceans Canada, Ottawa.

Heffernan, J. E., and Tawn, J. A. (2004). A conditional approach for multivariate extreme values (with discussion). *Journal of the Royal Statistical Society: Series B (Statistical Methodology)*, 66(3), 497–546.

Hersbach, H., Bell, B., Berrisford, P., Hirahara, S., Horányi, A., and Muñoz-Sabater, J. (2020). The ERA5 global reanalysis. *Quarterly Journal of the Royal Meteorological Society*, 146(730).

USACE (2002). *Coastal Engineering Manual (CEM): Engineer Manual 1110-2-1100*. US Army Corps of Engineers (USACE), Washington, D.C. (6 Volumes) pp.

Walker, I. J., and Barrie, J. V. (2006). Geomorphology and Sea-level Rise on one of Canada's Most Sensitive Coasts: Northeast Graham Island, British Columbia. *Journal of Coastal Research*, (39).